# Identifying risky components of display products for redesign considering indexes of user attention and design risky

Xiaozhen Lian[1], Liang Hou[1*], Wenbo Zhang[1], Husehng Yan[1,2], Ying Liu[3]

1 Department of Mechanical and Electrical Engineering, Xiamen University, Xiamen, 361102, China

2 Department of Consumer Quality, Tianma Microelectronics Co., Ltd, Xiamen, 361101, China

3 Institute of Mechanical and Manufacturing Engineering, Cardiff University, Cardiff, CF24 3AA, UK

[*]Corresponding authors. E-mail: hliang@xmu.edu.cn

## Abstract

Identifying risky components are crucial to improving product reliability in the final redesign of products. Design failure mode and effects analysis has become a prevalent application in product redesign as a useful risk assessment method. However, critical data, which contain failure causality relationships (FCRs) between failure modes, correlations among risk factors, and user attention index of the product component, are not considered. This study develops an improved approach for identifying the target risky components considering customer requirement, user attention, and FCRs based on the design risky component (DRC) and nonlinear optimization model. The DRC, which integrates the customer requirement level, quality test level, and failure risk information of product components, is proposed to represent the risk degree of product components. The nonlinear optimization models are constructed to derive the weights of risk factors and final redesign of product components. Firstly, a two-stage fuzzy quality function deployment is established to map the customer requirements under a trapezoidal fuzzy number. A local-global normalization measure is implemented to calculate the importance level of the user attention based on quality test data. Secondly, the FCRs of failure modes between or within product components is characterized by a directed network model. In this network, the failure modes are modelled as vertices, and the causality relationships among failure modes are modelled as directed edges. The values of the directed edges are characterized by weighted risk priority numbers, and the weight of risk factors is optimized by a nonlinear optimization model. Then, the FCRs incorporates the internal failure effect and the external failure effect, which are characterized by PROMETHEE Ⅱ with the net flow. A 0-1 optimization model with the maximum redesign value and resource constraints of product components is constructed to decide on the final redesign of target risky components. Finally, a real-world case of display product is conducted to demonstrate the validity and feasibility of the proposed approach. The results demonstrate that the proposed method is more effective in identifying risk components.

*Keywords:* Design failure mode and effects analysis; Fuzzy quality function deployment; Failure causality relationships; Design risky component; optimization model; Display products

# 1 Introduction

Product reliability (*PR*) is one of the key dimensions of the quality of products. New products are usually developed by improving existing products to meet customer requirements (*CRs*) and *PR*, which is particularly true for electronic products such as mobile phones, personal computers, and other intelligent products (Zhang et al. 2018; Jiao et al. 2021; Deng and Yuan 2021; Tang and Meng 2021). These products usually have high *CRs* for *PR*, leading to considerable delivery time (*DT*), engineering cost (*EC*), and technology risk (*TR*) during their redesign processes (Zhang et al. 2019). To improve *PR*, product redesign has become an important method in the process of new product research and development (Smith et al. 2012). Hence, the key issue of *PR* is to identify risky components (Ma et al. 2019; Zhou et al. 2021).

To identify risky components, the *CRs* are primarily considered (Shin et al. 2015; Geyer et al. 2018; Yan and Ma 2015), while the failure information from enterprises and customers, which is critical to improving the *PR*, is often ignored. To improve the *PR*, both components with low customer satisfaction and those with high failure risk must be identified considering the failure information. The requirements and preferences are usually included in the bill of materials, it is critical to understand the customer's preferences and failure risk of products to improve the *PR* in the redesign.

Conventionally, *CRs* are extracted as the input of quality function deployment (QFD) through those methods of customer surveys, questionnaires, and interviews (Zhang et al. 2019; Hou and Jiao 2020), which are used by designers to select product components (*PCs*) to be improved (Ma et al. 2019). QFD is generally utilized to extract design characteristics from *CRs* with subjective qualitative evaluation (Fazeli and Peng 2021). Failure mode and effects analysis (FMEA) is used to determine the failure risk of *PCs* to enhance the *PR* (Yucesan and Gul 2021). Failure modes (*FMs*) are prioritized based on a risk priority number (*RPN*), which is an arithmetic product of three risk factors (*RFs*), namely, severity (*S*), occurrence (*O*), and detection (*D*). Risk factor takes a discrete value from designers (Zhou et al. 2021), an *FM* with a large *RPN* value has a higher failure risk and greater priority to be redesigned. However, the traditional QFD and FMEA have been intensively criticized for their weaknesses and limitations in subjective and stochastic (Ma et al. 2019; Fazeli and Peng 2021; Wang et al. 2019;

Yu et al. 2021). Considerable efforts have been made to improve the QFD and FMEA to accommodate various engineering and design problems. For example, to improve the *PR*, a redesign framework was presented to support the conceptual design of complex products and systems based on a modified QFD and FMEA (Ma et al. 2019). In addition, similar approaches have been presented to solve different problems, such as performance improvement of service demand selection (Chen 2016), risk assessment with fuzzy information (Liang and Li 2021), and customer needs analysis (Xu et al. 2009). In these studies, the *CRs* and failure risk were incorporated into the QFD process by FMEA and was treated as a constraint in the risk evaluation model. The studies discussed above show that the failure information of the product is accessible and usable for the improvement of *PR*. However, the evaluation value of *CRs* and *PCs* were subjective and uncertain, and the causality relationships among the *FMs* of *PCs* received quite a little attention (Ma et al. 2017; Zhou et al. 2021). In the product lifecycle, the design and manufacturing are closely related to each other. Failure information of quality test data, obtained by enterprises and customers, can be utilized to identify risky components in the stage of product redesign. Nevertheless, those aforementioned studies have not jointly considered interdependencies (namely, the mapping relations from *CR*s to *PC*s, causalities among *FMs*, interactions among *RFs*, and correlations among *PCs*) in the QFD and FMEA.

As an effective reliability design method for identifying and eliminating potential failures in product design, manufacturing, and service processes (Huang et al. 2019), FMEA has been widely used in product design process (Zhou et al. 2021). Based on the application phases of FMEA, which can be divided into design FMEA (DFMEA), process FMEA (PFMEA), and service FMEA (SFMEA) (Chang and Wen 2010; Belu et al. 2013; Huang et al. 2019). The National Aeronautics and Space Administration adopted DFMEA in their product design processes in 1963 (Chang and Wen 2010). DFMEA is suitable for reliability improvement of products and plays a key role in risk prevention. DFMEA has become a prevalent application in product redesign as a useful risk assessment method, and those methods can also be applied to other types of FMEA due to FMEA's similarity in both contents and structure (Rivera et al. 2018; Huang et al. 2019; De et al. 2022). At present, DFMEA has become an integral part in product development of various industries, including aerospace, automotive, and precision mechanics (Sellappan et al. 2015; Rivera et al. 2018; Huang et al. 2019).

To identify target risky components for improving *PR*, an improved approach with fuzzy QFD (FQFD) and fuzzy DFMEA is proposed in this article. The main innovative points of the proposed method are concluded as follows: (1) An importance index of *PCs* and user attention is determined by a two-stage FQFD and a local-global normalization measure (LGNM), this index incorporates the preferences of customers and the interests of designers considering both subjective and objective data, and the uncertainty in the redesign process can be reduced effectively. (2) The design risky component (DRC) of *PCs* is defined and computed, the *DRC* incorporates the importance index, user attention index, and failure index, where the weight of the *RFs* is calculated by a nonlinear optimization model to modify the traditional RPN of DFMEA, and the risk components for redesign can be identified precisely. (3) The failure causality relationships (FCRs) among *FMs* between and within *PCs* are analyzed by the directed networks, the FCRs incorporates the internal failure effect (IFE) and the external failure effect (EFE), which are characterized by PROMETHEE Ⅱ with the net flow. Then, a 0-1 optimization model considering maximum redesign value (MRV) and resource constraints of *PCs* is constructed to decide on the final redesign of target risky components.

In summary, an improved FQFD and fuzzy DFMEA approach are developed to decide on the final redesign of *PCs* based on the indexes of user attention, design risky, and optimization model. The remainder of this paper is organized as follows. In Section 2, a brief review of related literature is presented. Then, in Section 3, the proposed approach for identifying risky components is introduced. Section 4 presents a real-world case of a display product to demonstrate the effectiveness of the proposed approach. Section 5 discusses the results of methods, and finally, Section 6 provides the conclusions.

## 2 Literature review

*PR* is often seen as a product quality attribute, which can be improved by identifying risky components. To ensure and improve *PR*, an organization must follow specific practices during the product design process. Acquiring *CRs* and identifying risky components in existing products have become an attractive research topic in recent years (Ma et al. 2019; Zhang et al. 2019; Zhou et al. 2021). Customers tend to evaluate the functions of products and describe their defects from users' perspectives (Smith et al. 2013; Mu et al. 2021). Moreover, designers

4

tend to acquire the *CRs* and failure information of products from the manufacturing process and product operation data (Hou and Jiao 2020; Yu et al. 2021). These evaluations, descriptions, and acquisitions of *CRs* and failure risk information are more reliable than interviews and brainstorming (Provost and Fawcett 2013; Kusiak 2017; Van et al. 2020; Xia et al. 2021).

## 2.1 Acquiring and mapping of customer requirements

Risky components can be identified through the analysis of *CRs*. The typical methods for acquiring *CRs* include brainstorming, interviews, market surveys, and online reviews (Serrano-Guerrero et al. 2015; Zhang et al. 2019; Mu et al. 2021; Zheng et al. 2021). As a fundamental step for identifying risky components in product design, mapping the *CRs* has been studied for many years (Xu et al. 2009; Smith et al. 2013; Mu et al. 2021). Xu et al. (2009) developed an analytical Kano model with a focus on customer needs analysis. In their study, two alternative mechanisms were proposed to provide decision support for product design, and Kano classifiers were used as tangible criteria for categorizing customer needs. Zhou et al. (2013) proposed an affective and cognitive design perspective to satisfy the latent needs of customers. By revealing the latent *CRs*, mass personalization aims to assist customers in making better adapt to delight the customer. The classical method for mapping *CRs* was QFD. Wu and Liao (2021) introduced a modified QFD framework to solve complex customer-oriented design problems regarding uncertain information on *CRs*, design requirements (*DRs*), and alternative performances. Li et al. (2006) developed a redesign approach to resolve the conflicts between *CRs* and component capability, which were represented by component-attribute pairs and resolved by changing the component attributes and replacing the defective components. Bovea and Wang (2007) introduced a redesign approach to incorporate environmental requirements into the product development process. They conducted a component-level analysis to determine the individual components to improve customer satisfaction. Smith et al. (2012) applied QFD to identify risky components to influence *CRs*, which stimulate innovation, and improve product quality. Ma et al. (2019) proposed a redesign approach that considers both *CRs* and product failure knowledge. In their study, QFD was employed to map the *CRs* to *PCs*.

QFD has become a popular method to map *CRs* in product design, engineering management, and service systems (Lee et al. 2015; Brenner and Uebernickel 2016). The methods discussed above mainly focus on *CRs* to identify risky components in the design

process and consider the failure information that is critical for improving *PR* (Ma et al. 2019; Zhang et al. 2019). However, the application of traditional QFD is limited by qualitative evaluation from designers, and the results are somewhat subjective. Therefore, to eliminate the subjectivity and uncertainty of the redesign procedure and practice application, a method that acquiring and mapping of CRs information needs to be improved. Meanwhile, an integrated method for the FCRs of *PCs* needs to be applied carefully.

**2.2 Identifying and analysis of failure risk knowledge**

Failure risk knowledge of product is a critical basis for evaluating reliability. For this, FMEA is a popular approach to identifying risky components based on various types of failure risk knowledge (Safari et al. 2016; Liang and Li 2021; Filz et al. 2021). Based on FMEA, when failure information is mapped to design knowledge, the target risky components are identified and product redesign can be implemented (Ma et al. 2019; Yucesan and Gul 2021; Bhattacharjee et al. 2022).

In this research area, Ma et al. (2019) proposed an approach for identifying the *PCs* to be improved by combining the QFD and FMEA for product redesign based on historical data. Zhou et al. (2021) proposed a novel FMEA-based approach to facilitate risk analysis of product redesign in an uncertain environment. Zhang and Chu (2011) proposed an approach for supporting the product conceptual design by combining FMEA. Liu et al. (2016a) introduced a new FMEA model based on a fuzzy digraph and matrix approach to improve the effectiveness of FMEA. By considering the *RFs* and their relative importance, a fuzzy digraph was developed for the optimum representation of interrelations. Liu et al. (2016b) presented the critical *RFs* of product design through mutual assessments and investigations using a novel FMEA for the reliability improvement of package design in a thin-film transistor product. Aguirre et al. (2021) revealed an integrated method, where FMEA, fuzzy sets, and dimensional analysis are combined to identify key risks. Zheng et al. (2021) proposed a novel approach that integrates a probabilistic graphic model named product defect identification and analysis model with the FMEA to derive product defect information from social media data.

FMEA has become a popular method to identify failure risk information in product design and engineering management (Ma et al. 2019; Zhou et al. 2021; Zheng et al. 2021; Bhattacharjee et al. 2022). As a useful risk assessment method, those methods of FMEA can

also be applied to other types of FMEA, such as, DFMEA and PFMEA, due to FMEA's similarity in both contents and structure (Rivera et al. 2018; Huang et al. 2019; De et al. 2022). At present, DFMEA has become an integral part in product development of various industries, including aerospace, automotive, and precision mechanics (Sellappan et al. 2015; Rivera et al. 2018; Huang et al. 2019). Those methods discussed above mainly focus on integrating of *RFs* to identify key failure modes in the process of product redesign and consider the failure information that is critical for improving *PR* (Ma et al. 2019; Zhang et al. 2019; Zhou et al. 2021). However, those studies discussed above neglect the subjective human intervention during *RFs* assessment, which leads to imprecision and incomplete failure risk information to identify risky components for *PR* regarding product redesign.

**2.3 Summary**

The above works shed light on the diversity of *CRs* and customer satisfaction, which help designers and manufacturers to gain insights on not only how customer satisfaction correlates with product improvements, but also how to design products for a particular group of customers. The data of *CRs* are applied in redesign through FQFD, while the data of *PR* are applied in redesign through DFMEA. However, owing to the objectivity or subjectivity of the data source from designers, the conventional acquiring methods of *CRs* and identification of risky components for product redesign are resulted dependent, leading to difficulties in determining hidden *CRs* and in implementing and identifying risky components of the redesign procedure. Compared with the subjective evaluation data, the quality test data during the manufacturing process can provide reliable results for product redesign. Thus, the quality test data is employed to identify risky components, which are jointly considered causalities among *FMs*, interactions among *RFs*, and correlations among *PCs*. Hence, an approach, which integrates objectivity and subjectivity data source from customers, designers, and the manufacturing process, needs to be explored for *PR*. The main works of this study are as follows:

(1) Based on the theory of trapezoidal fuzzy number (TrFN), a two-stage FQFD for converting the *CRs* to *DRs* and *PCs* is applied to reduce the ambiguity and uncertainty of mapping procedures to calculate the importance index of *PC*s. To eliminate the designers' subjectivity on the importance index *C*, a data mining method of local-global normalization measure (LGNM) is applied to calculate the user attention index of *PCs* based on quality test

data.

(2) Based on the fuzzy DFMEA, a nonlinear optimization model is constructed to derive the weight of *RFs* of *FMs* to calculate the weighted *RPN*. By considering the *FCRs* between and within *PCs*, a directed network model is constructed to obtain the failure index of product components. The failure index is divided into the IFE and EFE, which are obtained by PROMETHEE Ⅱ with the net flow.

(3) The index of *DRC* is proposed to model the risk degree of product components considering the importance index, the user attention index, and the failure index. A 0-1 optimization model of the target risky components is constructed to decide on the final redesign of *PCs* for *PR*. A real-world case of display products is conducted to demonstrate the validity and feasibility of the proposed approach.

## 3 The proposed approach

This section introduces the procedures and key techniques of the proposed approach in this paper. Firstly, the importance index of *CRs* and user attention index are calculated based on an improved FQFD (Ma et al. 2019) and LGNM (Zhang et al. 2019). Secondly, the weighted *RPN* of *FMs* is calculated based on a nonlinear optimization model. Then, the failure index of *PCs* is defined based on an improved directed network model and PROMETHEE Ⅱ (Molla et al. 2021). Finally, the target risky components of an existing product are constructed based on a 0-1 optimization model to decide on the final redesign *PCs* for *PR*.

In this study, the *DRC* is proposed to represent the risk degree of component of an existing product considering the objective data and subjective information. The *DRC* is defined:

$$DRC = C^{W_c} \cdot U^{W_u} + FI^{W_f} \tag{1}$$

where *C* represents the importance index of the *PCs* determined by a two-stage FQFD based on *CRs*; *U* denotes the user attention index, which modify the importance index of the *PCs*, is determined by the LGNM based on quality test data; *FI* represents the failure index determined by failure risk information based on directed network model and PROMETHEE Ⅱ. The $W_c$, $W_u$, and $W_f$ are the weight factors of *C*, *U*, and *FI*, respectively ($W_c + W_u + W_f = 1$). The weight factors represent the importance of the three indexes. The weight factors can be assigned by designers according to the design characteristics and parameter levels. For example, for

smartphones, which are characterized by changing *CRs* or user attention and involved high interactions with customers, $W_c$ and $W_u$ are assigned high values. For mechanical product, which is characterized by long operation life and high *PR*, $W_f$ is assigned a high value. To decide on the final redesign of risky components, a threshold *t* of the *DRC* must be predefined. Once the *DRC* of a component exceeds that of another, this component is identified for improvement. Usually, *t* is selected by decision makers according to the specific product case and constraints of redesign resources, including *DT*, *EC*, and *TR*. When sufficient redesign resources are available, a higher *t* can be selected to identify more target risky components. In contrast, when the redesign resources are insufficient, a lower *t* can be selected to identify fewer target risky components.

So far, the detailed calculating procedures of *C*, *U*, and *FI* are described in Sections 3.1 and 3.2, respectively. And the procedures for calculating *FCRs* and identifying target risky components are introduced in Sections 3.3 and 3.4. Thus, the flowchart framework of the proposed approach is depicted in Figure 1.
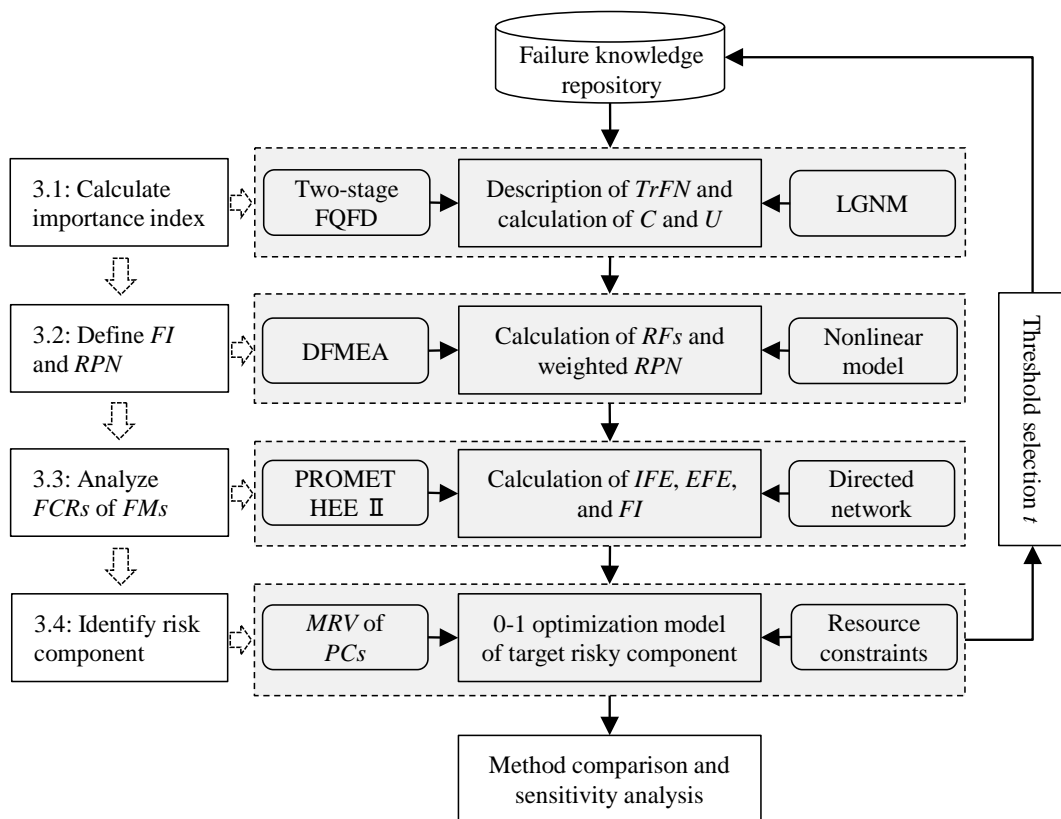


Figure 1 Workflow framework of the proposed approach

The flowchart framework of the proposed approach can be described as follows:

Subsection 3.1: According to *CRs* information and quality test data, the importance indexes of *C* and *U* can be calculated based on FQFD and LGNM.

Subsection 3.2: The *FI* and weight of *RFs* can be defined by the DFMEA and nonlinear optimization model.

Subsection 3.3: The *FCRs* of *FMs* within *PC* or between *PCs* can be analyzed based on the directed network model, and the values of the *IFE*, *EFE* and *FI* of *PC* can be calculated based on PROMETHEE Ⅱ with the net flow.

Subsection 3.4: According to the MRV and resource constraints of *PCs*, the target risky components can be identified to decide on the final redesign of *PCs* based on the 0-1 optimization model.

With the changes of design threshold *t*, different target risky components of *PCs* can be identified to improve the *PR*. Finally, the validity and feasibility of the proposed approach are verified by method comparison and sensitivity analysis.

## 3.1 Calculate *C* and *U* by fuzzy quality function deployment and local-global normalization measure

3.1.1 *Description of trapezoidal fuzzy number*

To reflect the imprecise nature semantics of the mapping relationships in FQFD, the interrelationship value of $R_{ih}$ between the *i*th *CR* and the *h*th *DR* is quantified by TrFN, which includes the following semantic terms: VL (very low), L (low), M (medium), H (high), and VH (very high). The interrelationship value of $R_{jh}$ between the *j*th *DR* and the *h*th *PC* is also quantified by semantic terms. All semantic terms are transformed into TrFN, as presented in Table 1 (Xia et al. 2006; Geyer et al. 2018).

Table 1 Semantic terms and TrFN

| Semantic terms | TrFN |
| --- | --- |
| Very low causality relationship (VL) | (0,0,1,2) |
| Low causality relationship (L) | (1,2,3,4) |
| Medium causality relationship (M) | (3,4,5,6) |
| High causality relationship (H) | (5,6,7,8) |
| Very high causality relationship (VH) | (7,8,9,10) |

The following is a detailed explanation of the TrFN (Xia et al. 2006). A quadruple $\widetilde{m} = (m_1, m_2, m_3, m_4)$ is called a TrFN if its membership function is:

$$u_{\widetilde{m}}(x) = \begin{cases} \dfrac{x - m_1}{m_2 - m_1} & (m_1 \leq x < m_2) \\ 1 & (m_2 \leq x \leq m_3) \\ \dfrac{m_4 - x}{m_4 - m_3} & (m_3 < x \leq m_4) \\ 0 & (x < m_1 \ or \ x > m_4) \end{cases} \tag{2}$$

where $m_1 \leq m_2 \leq m_3 \leq m_4$ are real numbers and reflect the fuzziness of the evaluation data. The closed interval $[m_2, m_3]$ is the mode of $\widetilde{m}$, while $m_1$ and $m_4$ are the lower and upper limits of $\widetilde{m}$, respectively. The Euclidean distance between two TrFNs $\widetilde{m} = (m_1, m_2, m_3, m_4)$ and $\widetilde{n} = (n_1, n_2, n_3, n_4)$ is defined (Wan and Dong 2015):

$$d(\widetilde{m}, \widetilde{n}) = \sqrt{\frac{1}{6}[(m_1 - n_1)^2 + 2(m_2 - n_2)^2 + 2(m_3 - n_3)^2 + (m_4 - n_4)^2]} \tag{3}$$

Here, the mean value method of the TrFN defuzzification process is given:

$$X = \frac{m_1 + m_2 + m_3 + m_4}{2} \tag{4}$$

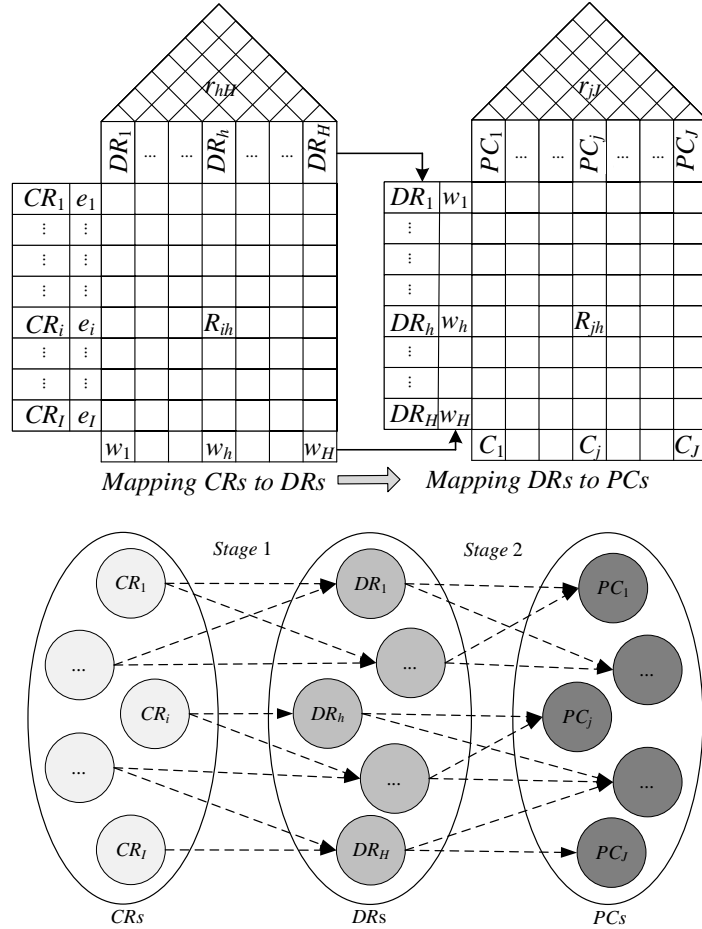3.1.2 *Calculation of C by fuzzy quality function deployment*



Figure 2 Two-stage FQFD for mapping *CRs* to *PCs*

A two-stage FQFD is applied to calculate the importance index of *CR*s to *PC*s, as shown in Figure 2. In this process, the *CRs* are mapped to calculate the *DRs*, which are mapped to calculate the importance index $C$ of the *PCs*.

As shown on the left of Figure 2 (Stage 1), the *CRs* are mapped to the *DRs*, where the $e_i$ $\sum_{i=1}^{I} e_i = 1$ ($i = 1, 2, \ldots, I$) represents the importance score of $CR_i$. Generally, the $e_i$ is predetermined by designers based on engineering practice. The interrelationship value $R_{ih}$ between the *i*th *CR* and the *h*th *DR* is quantified by TrFN. The interrelation $r_{hH}$ between *DRs* is quantified by TrFN. The $w_h$ ($h = 1, 2, \ldots, \tau, \ldots, H$) is the important weight of the *h*th *DR*, which is calculated using Equation (5):

$$\begin{cases} R_{ih}^{'} = \dfrac{\sum_{\tau=1}^{H} (R_{i\tau} \cdot r_{hH}^{'})}{\sum_{h=1}^{H} \sum_{\tau=1}^{H} (R_{i\tau} \cdot r_{hH}^{'})} \\ w_h = \sum_{i=1}^{I} e_i \cdot R_{ih}^{'} \end{cases} \tag{5}$$

where $R_{ih}^{'}$ is the normalized relationship value of $R_{ih}$ between the *i*th *CR* and the *h*th *DR* and is quantified using a TrFN.

As shown on the right of Figure 2 (Stage 2), the *DRs* are mapped to the *PCs*, the $\ddot{w}_h$ is the normalized importance weight ($w_h$) of $DR_h$. The $C_j$ is the importance index of the *j*th *PC* ($j = 1, 2, \ldots, J$), which is calculated using Equation (6):

$$C_j = \frac{\sum_{h=1}^{H} R_{jh} \cdot \ddot{w}_h}{\sum_{j=1}^{J} \sum_{h=1}^{H} R_{jh} \cdot \ddot{w}_h} \tag{6}$$

where $R_{jh}$ represents the normalized relationship value between the *h*th *DR* and *j*th *PC*, and $R_{jh}$ is quantified by TrFN. So far, the mapping relationships between *CR*s and *DR*s, as well as *DR*s and *PC*s, are determined.

3.1.3 *Calculation of U by local-global normalization measure*

To eliminate the enterprise designers' subjectivity on the importance index $C$, a data mining method is applied to calculate the user attention index $U$ of the *PCs* based on the quality test data during the manufacturing process. In this research, the LGNM is applied to evaluate the quantitative importance level for *PC*. Compared with subjective measures, the LGNM has some advantages because it uses three different terms (Zhang et al. 2019): local, global, and normalization. The global term reduces the effect of features that occur too often in all test

results of product quality. The normalization term mitigates the effect due to high term frequencies observed in all the tested products.

Here, the LGNM is applied to calculate the user attention $u_j$ ($j = 1, 2, …, J$) based on the quality test data during the manufacturing process, and $U_j$ is the normalized value of $u_j$:

$$
\begin{cases}
U_j = \dfrac{u_j}{\sum_{j=1}^{J} u_j} \\
u_j = \displaystyle\sum_{i=1}^{M} L_{ij} \cdot G_j \cdot Z_i
\end{cases}
\tag{7}
$$

where $L_{ij}$ is the local weight of the $j$th $PC$ in the $i$th quality test, $G_j$ is the global weight of the importance of the $j$th $PC$ in all quality tests, and $Z_i$ is the normalization factor to compensate for the discrepancies due to the lengths of the quality tests. The local test frequency $f_{ij}$ is defined as the number of occurrences of the $j$th $PC$ in the $i$th quality test. It can be calculated from the local negative quality $n_{ij}$ and positive quality $p_{ij}$ of the $j$th $PC$ in the $i$th quality test (yield and defect rates are derived from a statistical probability distribution). Then, the local factor $L_{ij}$ and local quality test frequency $f_{ij}$ are calculated:

$$
\begin{cases}
L_{ij} = log_2(1 + f_{ij}) \\
f_{ij} = n_{ij} + p_{ij}
\end{cases}
\tag{8}
$$

Then, the global quality test frequency $F_j$ (which can be calculated from the local qualities $n_{ij}$ and $p_{ij}$) is the frequency of the $j$th $PC$ on all test products. The global factors $G_j$ and $F_j$ are calculated by:

$$
\begin{cases}
G_j = 1 + \displaystyle\sum_{i=1}^{M} \dfrac{(f_{ij}/F_j)ln(f_{ij}/F_j)}{lnM} \\
F_j = \displaystyle\sum_{i=1}^{M} n_{ij} + \sum_{i=1}^{M} p_{ij}
\end{cases}
\tag{9}
$$

Then, the normalization factor $Z_i$ is calculated by:

$$
Z_i = 1 \Big/ \sqrt{\sum_{j=1} \left( L_{ij} \cdot G_j \right)^2}
\tag{10}
$$

## 3.2 Define failure index and weighted risk priority number

### 3.2.1 *Description of failure index by the directed network model*

Suppose a product has $J$ $PC$s, in which each $PC$ has various design parameter levels and is accompanied by different $FMs$ (i.e., $j_1$, …, $j_2$, …, $j_v$). In the conventional methods for

calculating the *DRC* of *PCs*, the *FCRs* between or within the *FMs* of *PCs* are usually ignored. In this study, the *DRC* is considered an important index determined by the DFMEA considering the *FCRs*. Here, the *FCRs* can be divided into *FMs* of the same *PC* and different *PCs*. Therefore, the failure index *FI* of *PCs* with *FCRs* is defined (Ma et al. 2019):

$$FI = IFE + EFE \tag{11}$$

where the *IFE* is the index of the internal failure effect corresponding to the *FCRs* within *FMs* of the same *PC*, and *EFE* is the index of the external failure effect corresponding to the *FCRs* among *FMs* of different *PCs*.

To model the *FCRs* within/among *FMs*, a directed network model can be constructed using the graph theory as $G = (V, E)$ (Ma et al. 2019; Zhou et al. 2021). For a graph $G = (V, E)$ with two sets, *V* and *E* are the vertex and edge of *G*, respectively. Here, a vertex represents an *FM*, and a directed edge represents the *FCRs* between *FMs*. For example, if $FM_A$ may cause $FM_B$, a directed edge between the two vertices of $FM_A$ and $FM_B$ needs to be drawn. The two *FMs* can also act as both causes and effects. In this process, the bill of materials and design records of *FMs* in the failure knowledge repository are also used to build the *FCRs*. The directed network model of *FCRs* for *PCs* among *FMs* (Ma et al. 2019; Zhou et al. 2021) is shown in Figure 3, where the rectangle represents a product, the squares represent the *PCs*, and the circles represent the *FMs*. The dotted lines indicate that a *PC* may have many *FMs* with different design parameter levels.
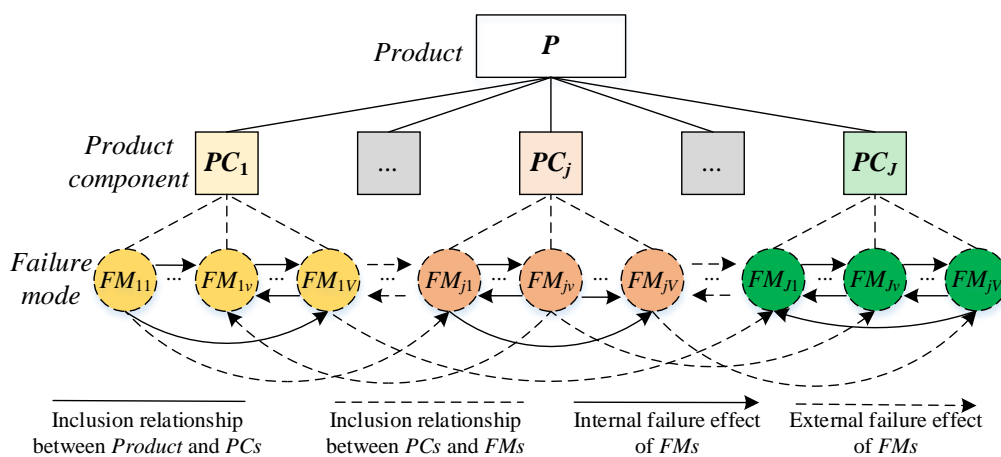


Figure 3 Directed network model of *FCRs* for *PCs* among *FMs*

In Figure 3, the *FCRs* among *FMs* are divided into two types (*IFE* and *EFE*), which are described using the directed solid curves with solid arrows and the directed dotted curves with

solid arrows, respectively. The directed edge represents the causality relationship between *FMs*, and the weight of the edge denotes the strength of this relationship. Usually, the assessment of the weight of the causality relationship is subjective and qualitatively described in semantic terms. Therefore, TrFN is used to describe the *FCRs* to reflect this imprecise nature.

3.2.2 *Calculation of weighted risk priority number by the nonlinear optimization model*

For a directed network model, the *RPN* can be determined to calculate the result of each $FM_{jv}$, as shown in Equation (19). With the help of a failure knowledge repository, the *RFs* of severity (*S*), occurrence (*O*), and detection (*D*) in the DFMEA can be obtained from Tables 2 to 4, which are presented in the section of *Appendix*. The rating scales of *S*, *O*, and *D* are converted into TrFN to reflect the imprecise nature of the subjective assessment, as indicated in Table 1. Meanwhile, the weights of *S*, *O*, and *D* need to be optimized. According to the principle of similarity measure (Selvachandran et al. 2018; Chutia and Gogoi 2018), the following optimization steps of weights are presented.

Step 1. The qualitative evaluation *RFs* (*S*, *O*, and *D*) is obtained using the linguistic variables listed in Table 1. Then, each $RF_{jv}^{P}$ is translated into a TrFN decision matrix as follows:

$$\left(\widetilde{\boldsymbol{RF}}_{j}\right)_{v}^{P} = \begin{bmatrix} \tilde{r}_{1}^{P} \\ \tilde{r}_{2}^{P} \\ \vdots \\ \tilde{r}_{V}^{P} \end{bmatrix} \tag{12}$$

where $\tilde{r}_{v}^{P} = (m_1, m_2, m_3, m_4)$ is a normalized TrFN, which denotes the $FM_j$ for each risk factor $\left(\widetilde{\boldsymbol{RF}}_{j}\right)_{v}^{P}$ ($j = 1, 2, ..., J$; $v = 1, 2, …, V$; $P = S, O, D$).

Step 2. Inspired by the principle of ideal solutions (Tian et al. 2018), the fuzzy reference preferences of the best and worst *RFs* are defined:

$$\begin{cases} \left(\widetilde{\boldsymbol{B}}_{j}\right)_{v} = (\tilde{b}_1, \tilde{b}_2, …, \tilde{b}_V) \\ \left(\widetilde{\boldsymbol{W}}_{j}\right)_{v} = (\widetilde{w}_1, \widetilde{w}_2, …, \widetilde{w}_V) \end{cases} \tag{13}$$

where $\tilde{b}_v$ and $\widetilde{w}_v$ are the normalization values of $b_v$ and $w_v$; $b_v = (7, 8, 9, 10)$ denotes the fuzzy preference of the best *RFs* of *O*, *S*, and *D*; and $w_v = (0, 0, 1, 2)$ represents the fuzzy preference of the worst *RFs* of *O*, *S*, and *D*.

Step 3. Inspired by the principles of the similarity measure (Chutia and Gogoi 2018), a nonlinear optimization model is constructed to derive the weights of *RFs* as follows:

$$
\begin{cases}
\displaystyle Min\, f(\omega_v^{P+}) = \sum_{v=1}^{V} \sum_{p=1}^{3} \left(\omega_v^{P+} d(\tilde{r}_v^P, \tilde{b}_v)\right)^2 \\[2em]
\displaystyle Max\, f(\omega_v^{P-}) = \sum_{v=1}^{V} \sum_{p=1}^{3} \left(\omega_v^{P-} d(\tilde{r}_v^P, \tilde{w}_v)\right)^2 \\[2em]
s.t. \begin{cases}
0 < \omega_v^{P+} < 1,\ 0 < \omega_v^{P-} < 1 \\[1em]
\displaystyle \sum_{P=1}^{3} \omega_v^{P+},\ \sum_{P=1}^{3} \omega_v^{P-} = 1 \\[1em]
0 \le d(\tilde{r}_v^p, \tilde{b}_v) \le d(\tilde{r}_v^p, \tilde{w}_v) \le 1
\end{cases}
\end{cases}
\tag{14}
$$

where for each risk factors $\left(\widetilde{RF}_j\right)_v^P$ ($j = 1, 2, ..., J$; $v = 1, 2, ..., V$; $P = S, O, D$); $\omega_v^{P+}$ represents the weight of the $RF_{jv}^P$ under $\left(\tilde{B}_j\right)_v = (\tilde{b}_1, \tilde{b}_2, ..., \tilde{b}_V)$; $\omega_v^{P-}$ represents the weight of the $RF_{jv}^P$ under $\left(\widetilde{W}_j\right)_v = (\tilde{w}_1, \tilde{w}_2, ..., \tilde{w}_V)$; $d(\tilde{r}_v^p, \tilde{b}_v)$ represents the Euclidean distances between $\left(\widetilde{RF}_j\right)_v^P$ and $\left(\tilde{B}_j\right)_v$; and $d(\tilde{r}_v^p, \tilde{w}_v)$ is the Euclidean distances between $\left(\widetilde{RF}_j\right)_v^P$ and $\left(\widetilde{W}_j\right)_v$, respectively. To simplify model (14), a Lagrange function is given as follows:

$$
Min\, F(\omega_v^{P+}, \omega_v^{P-}, \theta)
$$

$$
= \sum_{v=1}^{V} \sum_{p=1}^{3} \left(\omega_v^{P+} d(\tilde{r}_v^P, \tilde{b}_v)\right)^2 - \left(\omega_v^{P-} d(\tilde{r}_v^P, \tilde{w}_v)\right)^2 + 2\theta\left(\sum_{P=1}^{3} \omega_v^{P+} - 1\right) + 2\theta\left(\sum_{P=1}^{3} \omega_v^{P-} - 1\right)
\tag{15}
$$

Taking the partial derivative of Equation (15):

$$
\begin{cases}
\dfrac{\partial L(\omega_v^{P+}, \omega_v^{P-}, \theta)}{\partial \omega_v^{P+}} = 0 \leftrightarrow \sum_{P=1}^{3} \omega_v^{P+} \left(d(\tilde{r}_v^P, \tilde{b}_v)\right)^2 + \theta = 0 \\[1.2em]
\dfrac{\partial L(\omega_v^{P+}, \omega_v^{P-}, \theta)}{\partial \omega_v^{P-}} = 0 \leftrightarrow \sum_{P=1}^{3} \omega_v^{P-} \left(d(\tilde{r}_v^p, \tilde{w}_v)\right)^2 + \theta = 0 \\[1.2em]
\dfrac{\partial L(\omega_v^{P+}, \omega_v^{P-}, \theta)}{\partial \theta} = 0 \leftrightarrow \sum_{v=1}^{V} \omega^{P+} + \sum_{v=1}^{V} \omega_v^{P-} - 2 = 0
\end{cases}
\tag{16}
$$

Here, Equation (16) can be simplified:

$$
\begin{cases}
\omega_v^{P+} = \dfrac{\left(\sum_{v=1}^{V} \left(\sum_{p=1}^{3} \left(d(\tilde{r}_v^p, \tilde{b}_v)\right)^2\right)^{-1}\right)^{-1}}{\sum_{p=1}^{3} \left(d(\tilde{r}_v^p, \tilde{b}_v)\right)^2} \\[2em]
\omega_v^{P-} = \dfrac{\left(\sum_{v=1}^{V} \left(\sum_{p=1}^{3} \left(d(\tilde{r}_v^p, \tilde{w}_v)\right)^2\right)^{-1}\right)^{-1}}{\sum_{p=1}^{3} \left(d(\tilde{r}_v^p, \tilde{w}_v)\right)^2}
\end{cases}
\tag{17}
$$

Then, the comprehensive weight $\omega_v^P$ of S, O, and D can be derived:

$$
\omega_v^P = \frac{\omega_v^{P+} + \omega_v^{P-}}{2}
\tag{18}
$$

Here, according to the $\omega_v^P = (\omega_v^1, \omega_v^2, \omega_v^3)$ of $RFs$ (S, O, and D), the $RPN_v$ of each $FM_{jv}$ for each

$PC_j$ is presented:

$$RPN_v = S^{\omega_v^1} \cdot O^{\omega_v^2} \cdot D^{\omega_v^3} \qquad (19)$$

## 3.3 Analyze failure causality relationships and failure index by directed network model and PROMETHEE Ⅱ

### 3.3.1 *Calculation of the internal failure effect within a product component*

According to Equation (19), the $RPN_v$ of $FM_{jv}$ is regarded as the vertex of the directed network model. Inspired by the principle of PROMETHEE Ⅱ (Sun and Zhu 2017; Molla et al. 2021), the directed network model of *FCRs* for the *IFE* of a *PC* (as shown in Figure 4) can be calculated using the following steps.
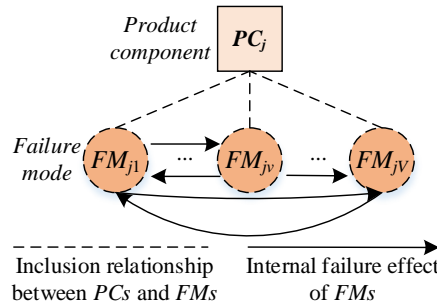


Figure 4 Directed network model of FCRs for the *IFE* of a *PC*

Step 1. Determine the preference function of *FMs* within a *PC* as follows:

$$\boldsymbol{F(PC_j)} = \begin{bmatrix} R_j^1 & \cdots & r_j^{1v} & \cdots & r_j^{1V} \\ \vdots & \vdots & \vdots & \vdots & \vdots \\ r_j^{v1} & \cdots & R_j^v & \cdots & r_j^{vV} \\ \vdots & \vdots & \vdots & \vdots & \vdots \\ r_j^{V1} & \cdots & r_j^{Vv} & \cdots & R_j^V \end{bmatrix} \qquad (20)$$

According to $\boldsymbol{F(PC_j)}$, failure modes $F_i$ and $F_t$ ($i, t = 1, 2, \ldots, v, \ldots, V$) are compared in pairs under different $RPN_v$. $R_j^v$ represents the *RPN* of the $v$th *FM* of the $j$th *PC*, and $r_j^{1v}, \ldots, r_j^{1V}$ denote the strength of fuzzy causality relationship among *FMs*. The result is a preference function of one over the other and is given as the accuracy value of an $RPN_v$. There are 6 common criteria for determining the preference function, where the Gaussian preference function has the characteristic of non-linear variation compared with others and is more in line with the actual decision-making environment. Hence, the Gaussian preference function is

chosen in this paper. The Gaussian preference function $p_j(F_i, F_t) \in [0, 1]$ between $F_i$ and $F_t$ is estimated as follows (Molla et al. 2021):

$$p(d) \begin{cases} 0 & d \le 0 \\ 1 - e^{-d^2/2\partial^2} & d > 0 \end{cases} \tag{21}$$

where $d = d_j(F_i, F_t) = RPN_i - RPN_t = F_i - F_t$, and $\partial = 0.2$.

Step 2. Calculate the weighted preference index of *FMs*:

$$H(F_i, F_t) = \sum_{v=1}^{V} r_j^v p_j(F_i, F_t) \tag{22}$$

Step 3. Estimate the leaving flow $L^+$, entering flow $L^-$, and net flow $L^+L^-$ of weighted preference index of $FM_i$:

$$\begin{cases} L^+(F_i) = \sum_{i=1}^{I} H(F_i, F_t) \\ L^-(F_i) = \sum_{i=1}^{I} H(F_t, F_i) \\ L^+L^-(F_i) = L^+(F_i) - L^-(F_i) \end{cases} \tag{23}$$

The leaving flow $L^+$ denotes the dominance of *FM* over other *FMs* and is a measure of the outranking character. The entering flow $L^-$ is a measure of the outranked character. The net flow $L^+L^-$ denotes the comprehensive dominance of *FM* between $L^+$ and $L^-$. Thus, the larger the value of the net flow $L^+L^-$, the higher is the ranking of *FM*. Then, the comprehensive *IFE* for $PC_j$ can then be calculated:

$$IFE_j = \sum_{i=1}^{V} L^+L^-(F_i) \tag{24}$$

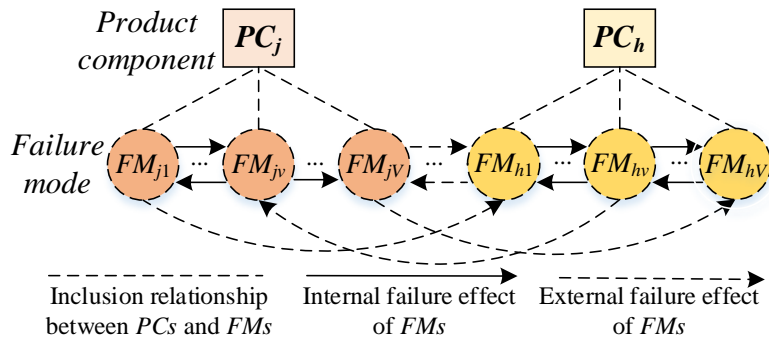3.3.2 *Calculation of the external failure effect and failure index*



Figure 5 Directed network model of FCRs for the *EFE* between any two *PCs*

Similarly, the *FMs* among different *PCs* interact with each other. For instance, panel extrusion

can cause display disorders in display products. Conventionally, existing FCRs analysis methods do not consider the interactions of *FMs* among different *PCs*. To interpret the *EFE* of the *FMs* among *PCs*, a directed network model comprising any two *PCs*, that is, $PC_j$ with $F_j$ *FMs* and $PC_h$ with $F_h$ *FMs*, is illustrated in Figure 5.

If the *j*th *FM* of $PC_j$ leads to the *h*th *FM* of $PC_h$, the directed dotted curves with solid arrows are drawn from *FM* node $F_{jv}$ to *FM* node $F_{hV}$ (denoted as $r_{jh}^{vV}$). To incorporate the *FCRs* content among *PCs* into the design process, the information matrix of the *EFE* between *PCs* is built:

$$F(PC_{jh}) = \begin{bmatrix} R_{jh}^1 & \cdots & r_{jh}^{1v} & \cdots & r_{jh}^{1V} \\ \vdots & \vdots & \vdots & \vdots & \vdots \\ r_{jh}^{v1} & \cdots & R_{jh}^v & \cdots & r_{jh}^{vV} \\ \vdots & \vdots & \vdots & \vdots & \vdots \\ r_{jh}^{V1} & \cdots & r_{jh}^{Vv} & \cdots & R_{jh}^V \end{bmatrix} \tag{25}$$

Then, the $EFE_j$ of $PC_j$ is defined:

$$EFE_j = \sum_{j=1, j \neq h}^{J} \sum_{j=1}^{jV} \sum_{h=1}^{hV} \sum_{v=1}^{V} r_{jh}^{vV} \cdot R_{jh}^v \tag{26}$$

where $R_{jh}^v$ and $R_{hj}^v$ are the *RPNs* of the *j*th *FM* of $PC_j$ and the *h*th *FM* of $PC_h$, respectively.

Thus, after defining and calculating the *IFE* and *EFE* of all *PCs*, the *FI* of *PCs* can be calculated. The normalized $FI_j$ of $PC_j$ is calculated:

$$FI_j = \frac{IFE_j + EFE_j}{\sum_{j=1}^{J} (IFE_j + EFE_j)} \tag{27}$$

### 3.4 Identify target risky components by 0-1 optimization model

So far, the normalized $DRC_j$ of $PC_j$, which is used to identify risky components of the product, is calculated. Because of the resource limitations of the primary constraints, such as *DT*, *EC*, and *TR*, a 0-1 optimization model is constructed to decide on the target risky components for the final redesign of *PCs*. The objective function of this optimization model is to achieve the *MRV* under various resource limitations. The 0-1 optimization model for identifying the target risky components of the product can be constructed as follows:

$$
\begin{cases}
MRV = Max \sum_{j=1}^{J} DRC_j \cdot x_j \\
s.t. \begin{cases}
max(DT_j \cdot x_j) \le T \\
\sum_{j=1}^{J} EC_j \cdot x_j \le C \\
\sum_{j=1}^{J} TR_j \cdot x_j \le R
\end{cases}
\end{cases}
\tag{28}
$$

where the threshold $t = (T, C, R)$; and the decision variable $x_j = 1$ if $PC_j$ is selected; otherwise, $x_j = 0$.

Assuming that all redesign tasks are conducted simultaneously, the final $DT$ is determined by the task requirement with the longest $DT$ among all the redesign tasks. The $EC$ is determined by the requirements of the market or customer. The $TR$ is defined as the quality fluctuation with the variables of reliability and serviceability (Gautam and Singh 2008):

$$
TR_j = RE_j \cdot SE_j \tag{29}
$$

where $RE$ and $SE$ are the changes in reliability and serviceability after the redesign, which can be obtained by a reliability test and service satisfaction evaluation by designers. The change in perceived value is applied to calculate $RE$ and $SE$ as follows (Zhang et al. 2019):

$$
\begin{cases}
RE_j = \sum_{j=1}^{J} P_j \cdot Q_{RE_j} + \sum_{j=1}^{J} \sum_{i=1}^{J} P_j \cdot Q_{RE_j} \cdot P_i \\
SE_j = \sum_{j=1}^{J} SE_j \cdot Q_{SE_j} + \sum_{j=1}^{J} \sum_{i=1}^{J} SE_j \cdot Q_{SE_j} \cdot SE_i
\end{cases}
\tag{30}
$$

where $P_j$ is binary for component change: $P_j=1$ if the $j$th component changes; otherwise, $P_j=0$. $P_i$ is the forced change from the coupled part to the $j$th component. $Q_{RE_j}$ is the change in the perceived value of the $j$th component due to the reliability change caused by redesign. The $SE$ can be defined and calculated similarly. Finally, the target risky component can then be identified from all candidate $PCs$ through the optimization model.

## 4 Case study

To verify the validity and feasibility of the proposed approach, a case study of product redesign is executed accurately to identify target risky components of the existing products. In this case

study, the key techniques of the proposed approach are implemented to improve *PR* based on objectivity and subjectivity data source from customers, designers, and the manufacturing process.

A real-world case of LCD-Module (LCM) for display products is presented to demonstrate the effectiveness of the proposed approach. The data for this case study were collected from a semiconductor manufacturing company located in the city of Xiamen, China. The company was planning to launch a series of quality renovations for the LCM to identify target risky components for the next-generation integrated panel module package with high *PR* to improve customer satisfaction. At the early design stage, the risky components must be identified because the given redesign tasks do not require changing all components. Because the LCM is composed of submodules, only the main *PCs* of LCM were selected for identification of the target risky components.
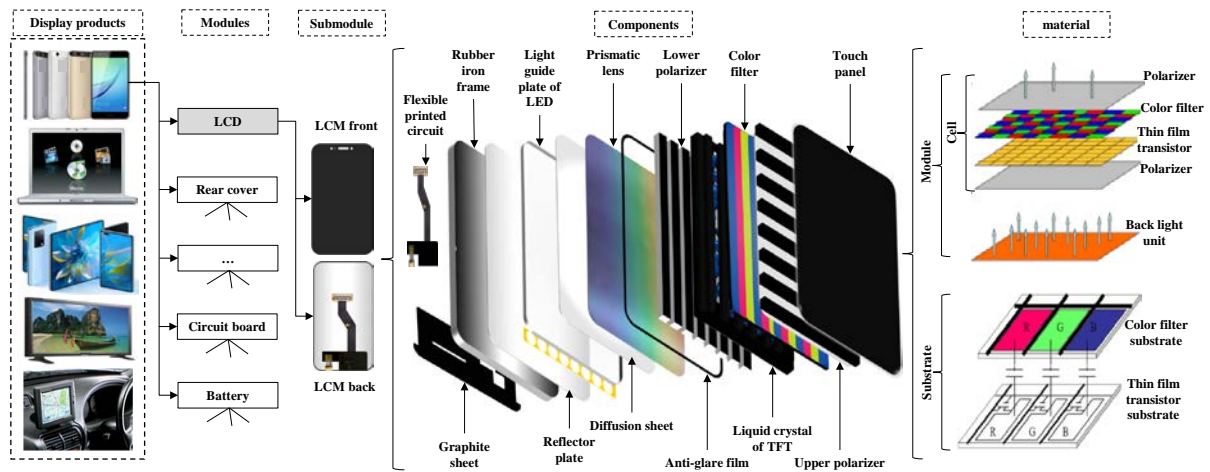


Figure 6 Essential structure of LCM of display products

The essential structure of LCM of display products is illustrated in Figure 6, and the descriptions of the *FMs* of *PCs* of LCM summarized in Table 5 were collected from the failure knowledge repository of the company.

Table 5 Description of *FMs* of risky *PCs*

| Risky *PCs* | Description of *FMs* |
|---|---|
| Optically clear adhesive: $PC_1$ | Bubbles are produced after pasting |
| Touch panel: $PC_2$ | Broken screen |
| Color filter: $PC_3$ | Larger color tolerance in the sample submission stage |
| Polarizer: $PC_4$ | There are cracks and color differences in the polarizer notch |
| Full cell: $PC_5$ | White screen shows character deviation, gamma offset, and residual shadow |

| | |
|---|---|
| Integrated circuit: $PC_6$ | ESD damage, flicker, and excessive power consumption |
| Flexible printed circuit: $PC_7$ | Line break, fracture, pressure deviation, and integrated circuit pin off |
| Backlight unit: $PC_8$ | Size deviation, film warping, edge bright line, and unsuitable selection of LED |
| Module: $PC_9$ | Offset light leakage, LED off, improper tray, fragments, reversed connection of FPC, and foreign bodies in the drum |
| Liquid crystal of TFT: $PC_{10}$ | Bad point line, picture flicker, extrusion light leakage, power consumption problem, dark line, and serrated display |

Note: TFT Thin film transistor; ESD Electro-static discharge; LED Light emitting diode; FPC Flexible printed circuit

## 4.1 Calculation of *C* and *U*

Above all, the subjective semantic terms were quantified to determine the importance index of *PCs*. By browsing the design repository of the LCM, the *CRs* include appearance, size, screen display, packing and transportation cost, electro-static discharge test, environmental and mechanical tests, and assembly time, denoted as six $CR_i$ ($CR_1$, $CR_2$, $CR_3$, $CR_4$, $CR_5$, and $CR_6$). The *DRs* includes film thickness, optical performance, power consumption, product reliability, three new technologies, and number of processes, symbolized as six $DR_i$ ($DR_1$, $DR_2$, $DR_3$, $DR_4$, $DR_5$, and $DR_6$). The weights of the six $CR_i$ were specified as $e_i$ = (0.181, 0.194, 0.208, 0.139, 0.167, and 0.111) based on historical statistical data of the total customer orders.
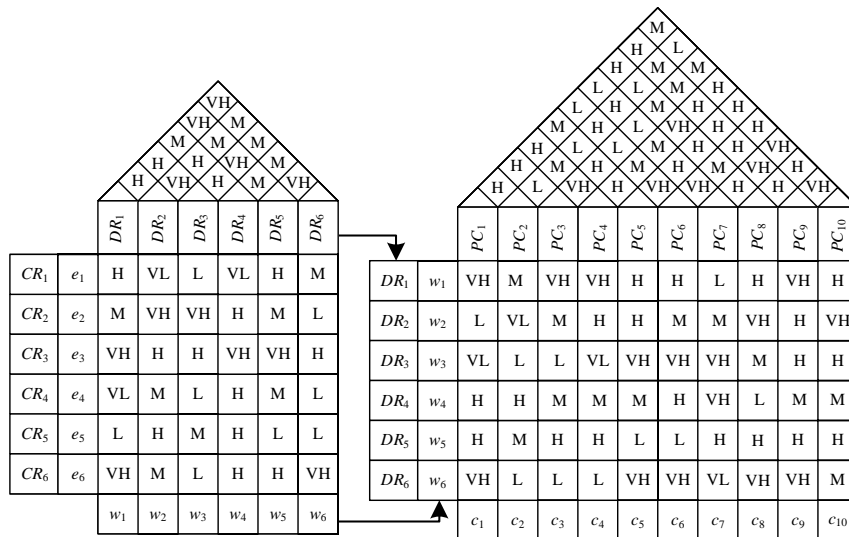


Figure 7 Mapping relationships between $CR_i$ and $DR_i$, as well as $DR_i$ and $PC_j$

The mapping relationships between $CR_i$ and $DR_i$, as well as $DR_i$ and $PC_j$, based on a two-stage FQFD are displayed in Figure 7. The designers' semantic evaluation was quantified according to TrFN (as listed in Table 1). To implement Equations (2)-(6), the weights of the $DR_i$ were set as $w_h$ = 0.1748, 0.1688, 0.1697, 0.1732, 0.1821, and 0.1314, and the subjective

importance index of $PC_j$ were $C_j$ = 0.0906, 0.0751, 0.0848, 0.1083, 0.1078, 0.0997, 0.1070, 0.1040, 0.1142, and 0.1087 according to $CRs$, respectively.

Secondly, the user attention index $U_j$ of $PC_j$ was analyzed based on quality test data from the manufacturing process. According to the feedback with quality test data under 31 risk attributes of 10 components, the local and global negative/positive opinion frequencies were calculated using Equations (8)-(10) to obtain the local and global preferences, and the normalized user attention index $U_j$ of $PC_j$ was calculated using Equation (7), as presented in Table 6, which is presented in the section of *Appendix*. Thus, the importance indexes of *C* and *U* were determined based on semantic evaluation and quality test data, respectively.

## 4.2 Calculation of weighted risk priority number

According to the failure information repository, the failure ranking of $RFs$ is described in Tables 2 to 4, and the assessment values of *S*, *O*, and *D* of $FMs$ are obtained in Table 7, which is presented in the section of *Appendix*. The assessment values of *S*, *O*, and *D* were converted to TrFN to reflect the imprecise nature of the subjective value. Then, the weights of *S*, *O*, and *D*, as well as the normalized $RPN$ (*n-RPN*) of $FMs$ were calculated using Equations (12)-(19), as listed in Table 8.

Table 8 Weights of $RFs$ and normalized $RPN$ of $FMs$

| $FM_{jv}$ | $w^S$ | $w^O$ | $w^D$ | $RPN$ | $n$-$RPN$ |
|---|---|---|---|---|---|
| $FM_{11}$ | 0.4565 | 0.0870 | 0.4565 | 6.2184 | 0.0482 |
| $FM_{21}$ | 0.5931 | 0.2035 | 0.2035 | 6.0339 | 0.0468 |
| $FM_{31}$ | 0.2513 | 0.2513 | 0.4975 | 4.1580 | 0.0322 |
| $FM_{41}$ | 0.2513 | 0.3744 | 0.3744 | 3.9046 | 0.0303 |
| $FM_{42}$ | 0.2513 | 0.3744 | 0.3744 | 3.9768 | 0.0308 |
| $FM_{51}$ | 0.3190 | 0.2566 | 0.4245 | 2.7036 | 0.0210 |
| $FM_{52}$ | 0.3190 | 0.2566 | 0.4245 | 4.0254 | 0.0312 |
| $FM_{53}$ | 0.3190 | 0.2566 | 0.4245 | 4.3859 | 0.0340 |
| $FM_{61}$ | 0.5033 | 0.2001 | 0.2967 | 4.3577 | 0.0338 |
| $FM_{62}$ | 0.5033 | 0.2001 | 0.2967 | 4.2522 | 0.0330 |
| $FM_{63}$ | 0.5033 | 0.2001 | 0.2967 | 4.2522 | 0.0330 |
| $FM_{71}$ | 0.6340 | 0.1485 | 0.2175 | 5.8309 | 0.0452 |
| $FM_{72}$ | 0.6340 | 0.1485 | 0.2175 | 5.2606 | 0.0408 |
| $FM_{73}$ | 0.6340 | 0.1485 | 0.2175 | 5.2606 | 0.0408 |
| $FM_{74}$ | 0.6340 | 0.1485 | 0.2175 | 5.8309 | 0.0452 |
| $FM_{81}$ | 0.3988 | 0.2024 | 0.3988 | 3.6436 | 0.0283 |
| $FM_{82}$ | 0.3988 | 0.2024 | 0.3988 | 3.6779 | 0.0285 |
| $FM_{83}$ | 0.3988 | 0.2024 | 0.3988 | 3.6436 | 0.0283 |

| | | | | | |
|---|---|---|---|---|---|
| $FM_{84}$ | 0.3988 | 0.2024 | 0.3988 | 3.6436 | 0.0283 |
| $FM_{91}$ | 0.3876 | 0.2729 | 0.3396 | 3.3538 | 0.0260 |
| $FM_{92}$ | 0.3876 | 0.2729 | 0.3396 | 3.9554 | 0.0307 |
| $FM_{93}$ | 0.3876 | 0.2729 | 0.3396 | 3.1864 | 0.0247 |
| $FM_{94}$ | 0.3876 | 0.2729 | 0.3396 | 4.2450 | 0.0329 |
| $FM_{95}$ | 0.3876 | 0.2729 | 0.3396 | 2.8527 | 0.0221 |
| $FM_{96}$ | 0.3876 | 0.2729 | 0.3396 | 3.6568 | 0.0284 |
| $FM_{101}$ | 0.4722 | 0.2272 | 0.3007 | 3.9620 | 0.0307 |
| $FM_{102}$ | 0.4722 | 0.2272 | 0.3007 | 3.6838 | 0.0286 |
| $FM_{103}$ | 0.4722 | 0.2272 | 0.3007 | 3.4365 | 0.0266 |
| $FM_{104}$ | 0.4722 | 0.2272 | 0.3007 | 3.8183 | 0.0296 |
| $FM_{105}$ | 0.4722 | 0.2272 | 0.3007 | 3.9620 | 0.0307 |
| $FM_{106}$ | 0.4722 | 0.2272 | 0.3007 | 3.7954 | 0.0294 |

## 4.3 Identification of failure index and design risky component

Based on the *FI* defined by Equation (11), the *FCRs* among *FMs* of *PCs* was constructed using the directed network model, which was divided into *IFE* and *EFE*. To save space, only $PC_7$ is shown in the calculation processes, tables, and figures.
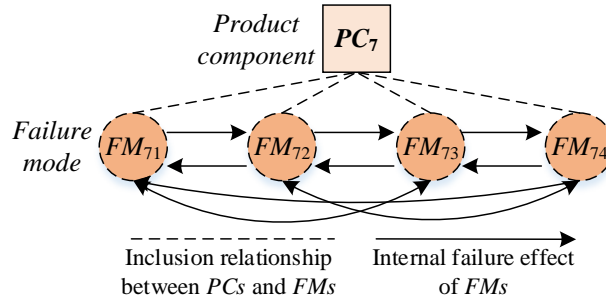


Figure 8 Directed network model *of FCRs* for the *IFE* of $PC_7$

Firstly, in the directed network model of *PCs*, the *IFE* of $PC_7$ is illustrated in Figure 8. Based on the *n-RPN* of *FMs* in $PC_7$, the preference function was obtained using Equations (20)-(21). Thus, the $L^+$, $L^-$, and $L^+L^-$ of the preference index of $FM_i$ were obtained using Equations (22)-(23). Then, the comprehensive *IFE* of $PC_7$ was obtained using Equation (24), as listed in Table 9.

Table 9 Values of the *EFE*, *IFE*, and *FI* for *PCs*

| Indices | $PC_1$ | $PC_2$ | $PC_3$ | $PC_4$ | $PC_5$ | $PC_6$ | $PC_7$ | $PC_8$ | $PC_9$ | $PC_{10}$ |
|---|---|---|---|---|---|---|---|---|---|---|
| $IFE_j$ | 0.0000 | 0.0000 | 0.0000 | 0.0000 | 0.0071 | 0.0000 | 0.0020 | 0.0000 | 0.0119 | 0.0018 |
| $EFE_j$ | 0.0024 | 0.0042 | 0.0026 | 0.0071 | 0.0071 | 0.0106 | 0.0123 | 0.0095 | 0.0124 | 0.0187 |
| $FI_j$ | 0.0216 | 0.0384 | 0.0235 | 0.0652 | 0.1296 | 0.0972 | 0.1301 | 0.087 | 0.2211 | 0.1862 |

Secondly, in the directed network model of *PCs*, the related EFE of $PC_7$ is displayed in Figure 9. Based on the *n-RPNs* of the *FMs* of $PC_7$, the *EFE* of $PC_7$ was obtained using

Equations (25)-(26), as presented in Table 9. Finally, the normalized *FI* of $PC_7$ was obtained

using Equation (27), as listed in Table 9.



Figure 9 Directed network model of *FCRs* for the *EFE* of $PC_7$ among *other PCs*

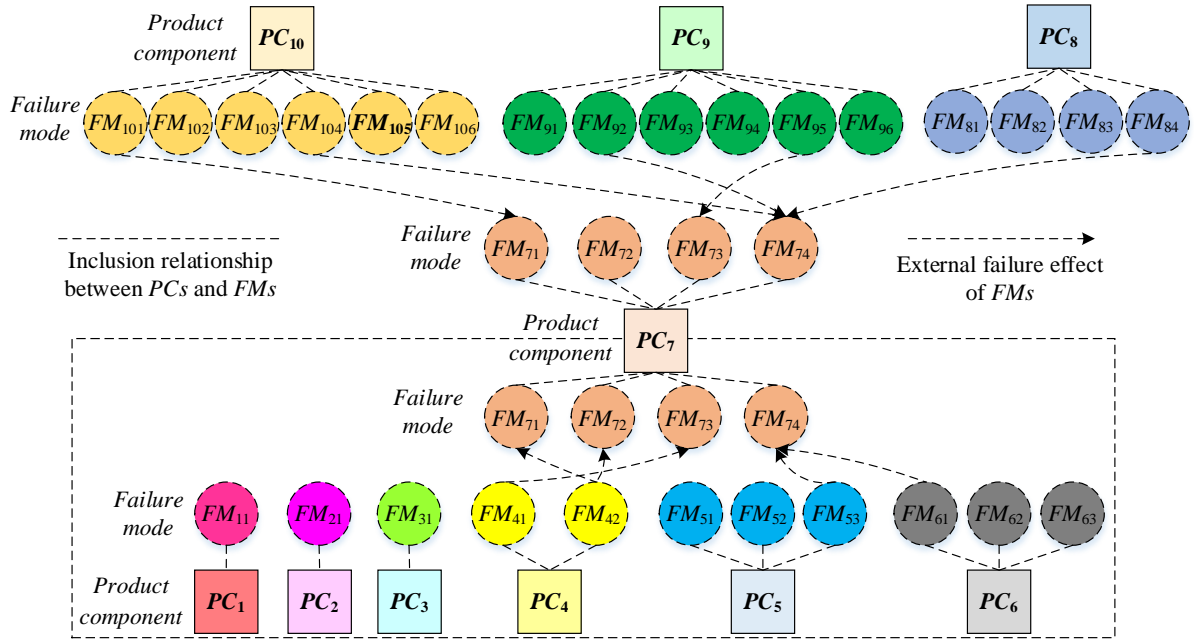Similarly, the $FI_j$ values of the other *PCs* are presented in Table 9. Here, the weights of *C*,

*U*, and *FI* are specified as $(W_c, W_u, W_f) = (0.25, 0.25, 0.5)$. Then, the *DRC* of all *PCs* were

calculated using Equation (1), as listed in Table 10. The rank of *PCs* according to the *DRC* is

presented in Table 10. Obviously, the rankings of *PCs* are different because of the different

weights of indexes (*C*, *U*, and *FI*) and calculation methods. These results with different weights

and methods are discussed further in Sections 5.1 and 5.2.

Table 10 Values of *DRC* of all *PCs*

| Index | $PC_1$ | $PC_2$ | $PC_3$ | $PC_4$ | $PC_5$ | $PC_6$ | $PC_7$ | $PC_8$ | $PC_9$ | $PC_{10}$ |
|---|---|---|---|---|---|---|---|---|---|---|
| $C_j$ | 0.0906 | 0.0751 | 0.0848 | 0.1083 | 0.1078 | 0.0997 | 0.1070 | 0.1040 | 0.1142 | 0.1087 |
| $U_j$ | 0.0966 | 0.0931 | 0.0947 | 0.0929 | 0.0983 | 0.0827 | 0.0837 | 0.0974 | 0.1371 | 0.1135 |
| $FI_j$ | 0.0216 | 0.0384 | 0.0235 | 0.0652 | 0.1296 | 0.0972 | 0.1301 | 0.087 | 0.2211 | 0.1862 |
| $DRC_j$ | 0.4528 | 0.4851 | 0.4526 | 0.5720 | 0.6808 | 0.6131 | 0.6683 | 0.6122 | 0.8239 | 0.7648 |
| Ranking | 9 | 8 | 10 | 7 | 3 | 5 | 4 | 6 | 1 | 2 |

## 4.4 Identification of target risky components

After obtaining the *DRC* of all *PCs*, according to project information and resource limitations,

the *DT*, *EC*, and maximum *TR* were selected as 100 h, \$3000, and 40%, respectively. Thus, the

threshold $t=(100, 3000, 40\%)$. The optimization model of the target risky component is

represented as follows:

$$\begin{cases} MRV = Max \sum_{j=1}^{10} DRC_j \cdot x_j \\ s.t. \begin{cases} Max_{10}(DT_j \cdot x_j) \leq 100 \\ \sum_{j=1}^{10} EC_j \cdot x_j \leq 3000 \\ \sum_{j=1}^{10} TR_j \cdot x_j \leq 40\% \end{cases} \end{cases} \qquad (31)$$

By searching for the optimal solutions considering different weights of $C$, $U$, and $FI$, the ranking of target risky components for the redesign were identified from alternative $PCs$, as presented in Table 11. From Table 11, $PC_9$ was selected under three situations with different weights of $C$, $U$, and $FI$. Similarly, in the ranking under $C$, $FI$, and $DRC$, $PC_9$ has the highest failure risk among all $PCs$.

Table 11 Identification ranking of target risky components

| Ranking | $W = (0.4, 0.4, 0.2)$ | $W = (0.25, 0.25, 0.5)$ | $W = (0.1, 0.1, 0.8)$ |
|---|---|---|---|
| 1 | $PC_9$ | $PC_9$ | $PC_9$ |
| 2 | $PC_{10}$ | $PC_{10}$ | $PC_{10}$ |
| 3 | $PC_5$ | $PC_5$ | $PC_5$ |
| 4 | $PC_7$ | $PC_7$ | $PC_7$ |

## 5 Discussions

To verify the shortcomings of the traditional method, a comparison study and sensitivity analysis were conducted to demonstrate the superiority of the proposed approach. An in-depth discussion of the proposed approach is carried out.

### 5.1 Comparison study

5.1.1 *Comparison between C, U, failure index, and design risky component*

The ranking result of $PCs$ with $C$, $U$, $FI$, and $DRC$ is presented in Figure 10. Some observations on the ranking results are summarized as follows:
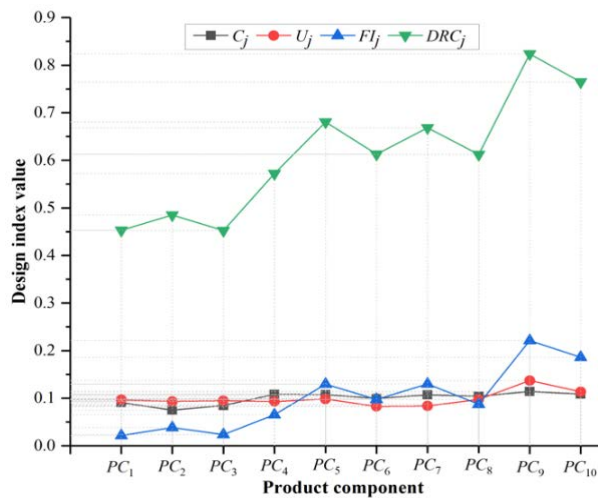


Figure 10 Comparisons of ranking results with four design indices

(1) $PC_9$ has the highest ranking among all $PCs$ based on four design indices $DRC$, $FI$, $U$, and $C$. The rankings with respect to $DRC$, $FI$, $U$, and $C$ are $PC_9 > PC_{10} > PC_5 > PC_7 > PC_6 > PC_8 > PC_4 > PC_2 > PC_1 > PC_3$; $PC_9 > PC_{10} > PC_7 > PC_5 > PC_6 > PC_8 > PC_4 > PC_2 > PC_3 > PC_1$; $PC_9 > PC_{10} > PC_5 > PC_8 > PC_1 > PC_3 > PC_2 > PC_4 > PC_7 > PC_6$; and $PC_9 > PC_{10} > PC_4 > PC_5 > PC_7 > PC_8 > PC_6 > PC_1 > PC_3 > PC_2$, respectively. Based on four design indices, except for $PC_9$ and $PC_{10}$, the rankings of the other $PCs$ are different. The main reason for this is that different methods have different computational emphases with evaluation preferences in terms of extremum data and weights of attributes. For example, based on $U$, for $PC_4$, the smallest of the global factor $G_j$ changes the results of $U$ among the 31 risk attributes of 10 components.

(2) The variation tendency of the ranking results of four design indices is clear: the fluctuations of the design indices $U$ and $C$ among $PCs$ are not obvious; therefore, it is difficult for decision-makers to prioritize the risky components. In contrast, the indices $DRC$ and $FI$ can satisfactorily depict the priorities of $PCs$. design indices

### 5.1.2 *Comparison between failure index, design risky component, and traditional risk priority number*

The comparison results of $FI$, $DRC$, and traditional $RPN$ (Ma et al. 2019) are presented in Table 12. Based on traditional $RPN$, $PC_{10}$ is the main risky component, which is completely different from the result based on $FI$ and $DRC$. The main reason for this is that traditional $RPN$ only considers the $FMs$ of $PCs$ without the FCRs of $FMs$ and preferences from designers and customers.

Table 12 Comparison results of *RPN*, *FI*, and *DRC*

| Index | $PC_1$ | $PC_2$ | $PC_3$ | $PC_4$ | $PC_5$ | $PC_6$ | $PC_7$ | $PC_8$ | $PC_9$ | $PC_{10}$ |
|---|---|---|---|---|---|---|---|---|---|---|
| *RPN* | 0.0482 | 0.0468 | 0.0322 | 0.0611 | 0.0862 | 0.0997 | 0.1720 | 0.1133 | 0.1648 | **0.1757** |
| *Ranking* | 8 | 9 | 10 | 7 | 6 | 5 | 2 | 4 | 3 | **1** |
| *FI* | 0.0216 | 0.0384 | 0.0235 | 0.0652 | 0.1296 | 0.0972 | 0.1301 | 0.087 | **0.2211** | 0.1862 |
| *Ranking* | 10 | 8 | 9 | 7 | 4 | 5 | 3 | 6 | **1** | 2 |
| *DRC* | 0.4528 | 0.4851 | 0.4526 | 0.5720 | 0.6808 | 0.6131 | 0.6683 | 0.6122 | **0.8239** | 0.7648 |
| *Ranking* | 9 | 8 | 10 | 7 | 3 | 5 | 4 | 6 | **1** | 2 |

### 5.1.3 *Comparison between different methods*

The traditional QFD method (Chen 2016) was employed to identify risky components for the comparative study. The comparison results of QFD (subjective assessment), $C \cdot U$ (Equation 1),

and *DRC* (Equation 1) are listed in Table 13.

Table 13 Comparison results between QFD, *C•U*, and *DRC*

| Index | $PC_1$ | $PC_2$ | $PC_3$ | $PC_4$ | $PC_5$ | $PC_6$ | $PC_7$ | $PC_8$ | $PC_9$ | $PC_{10}$ |
|-------|--------|--------|--------|--------|--------|--------|--------|--------|--------|-----------|
| *QFD* | 0.0906 | 0.0751 | 0.0848 | 0.1083 | 0.1078 | 0.0997 | 0.1070 | 0.1040 | **0.1142** | 0.1087 |
| *Ranking* | 8 | 10 | 9 | 3 | 4 | 7 | 5 | 6 | **1** | 2 |
| *C•U* | 0.4585 | 0.5063 | 0.4615 | 0.5723 | 0.6791 | 0.6210 | 0.6731 | 0.6122 | **0.7937** | 0.7645 |
| *Ranking* | 10 | 8 | 9 | 7 | 3 | 5 | 4 | 6 | **1** | 2 |
| *DRC* | 0.4528 | 0.4851 | 0.4526 | 0.5720 | 0.6808 | 0.6131 | 0.6683 | 0.6122 | **0.8239** | 0.7648 |
| *Ranking* | 9 | 8 | 10 | 7 | 3 | 5 | 4 | 6 | **1** | 2 |

Some differences exist between the results achieved based on QFD, *C•U*, and *DRC*: (1) the rank of $PC_4$ dropped from the third for QFD to the seventh for *DRC* and *C•U*; (2) the rank of $PC_5$ jumped from the fourth for QFD to the third for *DRC* and *C•U*; (3) the rank of $PC_7$ jumped from the fifth for QFD to the fourth for *DRC* and *C•U*; (4) the rank of $PC_6$ jumped from the seventh for QFD to the fifth for *DRC* and *C•U*; (5) the rank of $PC_1$ dropped from the eighth for QFD to the ninth for *DRC* and the tenth for *C•U*; (6) the rank of $PC_3$ dropped from the ninth for QFD and *C•U* to the tenth for *DRC*; (7) the rank of $PC_2$ jumped from the tenth for QFD to the eighth for *DRC* and *C•U*.

There are two reasons for the above ranking differences. (1) The QFD considers the preferences of designers and customers without the *FCRs* of *FMs* of *PCs*. (2) Only the subjective semantic term is given by designers, without the objective quality test data. It is noteworthy that the proposed approach can degenerate into one of the above methods or more general indices when the data are insufficient or unavailable. For instance, if the quality test data are unavailable, the *FCRs* among *FMs* and *DRC* of *PCs* are insufficient.

**5.2 Sensitivity analysis**

5.2.1 *Sensitivity analysis for $W_c$, $W_u$, and $W_f$*

In determining the *DRC* of *PCs*, the weights of *C*, *U*, and *FI* are predetermined by the designer based on experience and preference. Different designers may have different preferences for the weights of *C*, *U*, and *FI*, which may affect the final redesign of *PCs*.

To verify the robustness of the proposed approach, a sensitivity analysis was performed by changing the values of $W_c$, $W_u$, and $W_f$, where $W_c + W_u + W_f = 1$ and $W_c = W_u$. The influence of $W_c$, $W_u$, and $W_f$ on the *DRC* is depicted in Figure 11. With the changes in $W_f$, the *DRC* of *PCs* fluctuates stably. When $W_f = 0.5$, the ranking of *PCs* is the same as that of the *DRC* in

Figure 10. When $W_f = 0$, the ranking of the *DRC* is indistinguishable. Overall, the influence of the weights on the ranking is insignificant. However, the *DRC* for all *PCs* gradually increases with changes in $W_f$ (compared to $W_f = 0.5$). Furthermore, a larger $W_f$ means that the designers pay more attention to the *DRC* to improve the *PR*.
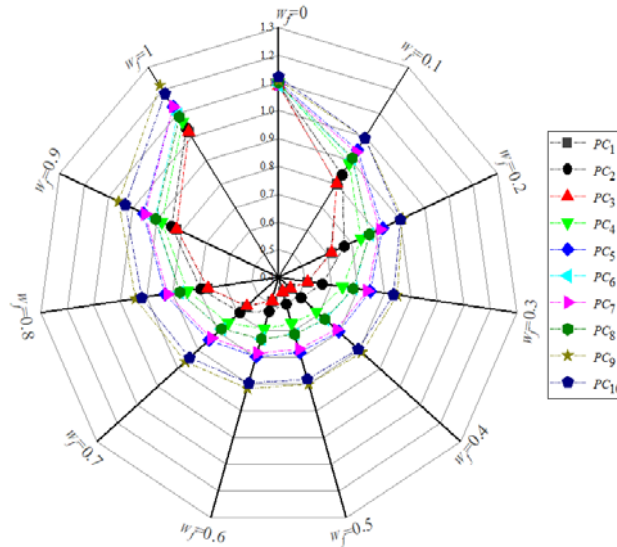


Figure 11 *DRC* of *PCs* with different weights of $W_f$

### 5.2.2 Sensitivity analysis for the threshold value t

Depending on the engineering practice, different companies may give different *t* values (Zhang et al. 2019), which may affect the final redesign of the target risky components. To verify the effectiveness of the proposed optimization model of target risky components, sensitivity analysis is carried out by changing the threshold value *t*. However, because changes in weights ($W_c$, $W_u$, and $W_f$) can also result in different *DRC*, changes in the target risky components with different *t* under different weights were also made, as displayed in Table 14. From Table 14, the following conclusions can be drawn:

Table 14 Target risky components with changes in *t* under different *W*

| *Threshold* | *Ranking* | *W* = (0.4, 0.4, 0.2) | *W* = **(0.25, 0.25, 0.5)** | *W* = (0.1, 0.1, 0.8) |
|---|---|---|---|---|
| | 1 | $PC_9$ | $PC_9$ | $PC_9$ |
| $t = (90, 2500, 35\%)$ | 2 | $PC_{10}$ | $PC_{10}$ | $PC_{10}$ |
| | 3 | $PC_5$ | $PC_5$ | $PC_5$ |
| | 1 | $PC_9$ | $PC_9$ | $PC_9$ |
| | 2 | $PC_{10}$ | $PC_{10}$ | $PC_{10}$ |
| $t = (100, 3000, 40\%)$ | 3 | $PC_5$ | $PC_5$ | $PC_5$ |
| | 4 | $PC_7$ | $PC_7$ | $PC_7$ |
| $t = (120, 3500, 45\%)$ | 1 | $PC_9$ | $PC_9$ | $PC_9$ |
| | 2 | $PC_{10}$ | $PC_{10}$ | $PC_{10}$ |

| 3 | $PC_5$ | $\mathbf{PC_5}$ | $PC_5$ |
| 4 | $PC_7$ | $\mathbf{PC_7}$ | $PC_7$ |
| 5 | $PC_6$ | $\mathbf{PC_6}$ | $PC_6$ |
| 6 | $PC_8$ | $\mathbf{PC_8}$ | $PC_8$ |

(1) When $t$ increases from (90, 2500, 35%) to (120, 3500, 45%) under fixed $W_c$, $W_u$, and $W_f$, the number of target risky components increases. For example, when $W = (0.25, 0.25, 0.5)$, the number of target risky components decreases from six to three as $t$ decreases from (120, 3500, 45%) to (90, 2500, 35%). This means that more target risky components will be identified for final redesign when resources are more plentiful.

(2) When $W$ changes from (0.4, 0.4, 0.2) to (0.1, 0.1, 0.8) under a fixed $t$, the identification results of target risky components are stable. For example, when $t = (90, 2500, 35\%)$, the target risky components are $PC_9$, $PC_{10}$, and $PC_5$ as $W$ changes from (0.4, 0.4, 0.2) to (0.25, 0.25, 0.5) or (0.1, 0.1, 0.8). This means that the target risky components for the final redesign are stable even when the values of $W_c$, $W_u$, and $W_f$ vary.

Furthermore, the identification results of the target risky components differ under different thresholds $t$; thus, the target risky components can be varied by setting different $t$. Moreover, the updated feedback from the failure knowledge repository can be obtained to improve the yield and reliability of product redesign. And in turn, meet the needs of customers and companies.

## 6 Conclusions

Traditional methods, such as QFD and FMEA, identify risky components based merely on *CRs* or failure information. However, the quality test data during the manufacturing process and *FCRs* among *FMs* must be considered as inputs to decide on the final redesign of *PCs*. Therefore, the *CRs* information, failure risk knowledge, and quality test data were integrated into this study to identify the target risky components based on an improved FQFD, fuzzy DFMEA, index of *DRC*, and optimization models. The contributions of this study are as follows:

(1) A systematic approach for identifying target risky components is proposed by integrating FQFD, DFMEA, *DRC*, and optimization models considering the subjective and objective data. Based on TrFN, a two-stage FQFD for converting the *CRs* to *DRs* and *PCs* is

applied to reduce the ambiguity and uncertainty of assessment. Using LGNM that can combine with the measure *C* of *PCs* to eliminate the subjectivity of the importance index, the objective user attention *U* of *PCs* is determined based on quality test data.

(2) A nonlinear optimization model is constructed to derive the weight of *RFs* of *FMs* to calculate the weighted *RPN* based on the failure knowledge repository. By considering the *FCRs* of *FMs* within and between *PCs*, a directed network model is constructed to obtain the *FI*, which is divided into *IFE* and *EFE*. The values of *IFE* and *EFE* are obtained by PROMETHEE Ⅱ with the net flow. And a 0-1 optimization model considering MRV and resource constraints of *PCs* is constructed to decide on the final redesign of target risky components.

From the case study of identifying the target risky components for the redesign of LCM, the proposed approach demonstrated its validity and feasibility in dealing with the redesign of display products. Several research directions need to be explored in the future: (1) *CRs* can be integrated into the DFMEA by constructing an identification model. The model can enable the DFMEA to classify *FMs* and *RFs* according to customer preferences (Lin et al. 2021). (2) The proposed approach can be further improved by considering more data based on new technologies (Zhang et al. 2021), for example, the multiple-view algorithm can be used to combine multiple information (such as manufacturing data, product maintenance data, function degradation data, and designer preferences) (Hou and Jiao 2020) from *RFs* and *FMs* of products for implementing the final redesign *PCs*.

## Appendix

Related Tables are presented as follows:

Table 2 Description of severity (*S*)

| Rating | Description |
| --- | --- |
| VH: Does not meet safety requirements | Potential failure consequences affect the safety or do not comply with government regulations, and failure occurs without warning. |
| | Potential failure consequences affect the safety or do not comply with government regulations, and failure occurs at the time of warning. |
| H: Loss or reduction of basic functions | Loss of basic function after failure (product cannot operate but does not affect safety). |
| | Basic function degradation (product is functional, but the function level is reduced). |
| | Loss of secondary functions. |

| | |
|---|---|
| M: Loss or reduction of secondary functions | Weakening of secondary functions. |
| L: Other dysfunctions | Appearance, noise, etc. do not meet requirements and are perceived by majority of customers ($> 75\%$). |
| | Appearance, noise, etc., do not meet the requirements and are perceived by many customers ($50\%$). |
| | Appearance, noise, etc. do not meet the requirements and are perceived by discerning customers ($< 25\%$). |
| VL: Without effects | There is no discernible effect. |

Table 3 Description of occurrence (*O*)

| Rating | The frequency of occurrence of causes within the reliability and life of the product. |
|---|---|
| VH: Very high | New technology/design with no history ($\cong 1/10$). |
| H: High | Failure is inevitable for new designs, new applications or changes in service life/operating conditions ($\geq 1/20$). |
| | Failure is possible for new designs, new applications or changes during service life/operating conditions ($\geq 1/50$). |
| | Failure is uncertain for new designs, new applications or changes in service life/operating conditions ($\geq 1/100$). |
| M: Medium | Similar designs (with reference objects), or frequent failures in design simulations and tests ($\geq 1/200$). |
| | Similar designs (with reference objects), or occasional failures in design simulations and tests ($\geq 1/500$). |
| | Similar designs (with reference objects), or individual failures in design simulations and tests ($\geq 1/1000$). |
| L: Low | Nearly identical designs or only isolated failures during design simulations and tests ($\cong 1/2000$). |
| | Almost identical designs or no failures were observed during design simulations and tests ($\leq 1/10000$). |
| VL: Very low | Failures can be eliminated through preventive control ($\cong 1/100000$). |

Table 4 Description of detection (*D*)

| Rating | Evaluation criteria: the possibility of discovery by design control. |
|---|---|
| VH: No chance of detection or easy detection at any stage | No existing design controls cannot be detected or analyzed. |
| | Design analysis has weak detection ability, virtual analysis (e.g., computer-aided engineering) is not associated with desired actual operating conditions. |
| H: After the design is finalized before it goes into production | After the design is finalized and before production, verify the product using pass/fail tests (test the product against acceptance criteria). |
| | After the design is finalized and before production, the product is validated by trial-to-failure testing (testing the product until failure occurs). |

| | | | |
|---|---|---|---|
| | After the design is finalized before putting into production, the product is verified by an ageing test and reliability test. | | |
| M: Before the design is finalized | Validation of products using passed/failed tests (reliability tests, development/validation tests) before design finalization. | | |
| | Verify product through the trial-to-failure test before final design (e.g., continue to test until leakage, bending, cracking, etc.). | | |
| | Before the design is finalized, the product is verified and confirmed by instrument measurement and ageing test. | | |
| L: Virtual analysis | The detection capability of design analysis/detection control is very strong, and virtual analysis (e.g., computer-aided engineering, optical simulation.) is highly relevant to the desired actual operating conditions. | | |
| VL: Can be prevented without detection | Failure causes or failure modes will not occur through adequate prevention by design solutions, such as proven design standards, best practices, or common materials. | | |

Table 6 User attention index $U_j$ of $PC_j$

| PCs | Risk attributes | Local preference | | | Global preference | | | Index |
|---|---|---|---|---|---|---|---|---|
| | | $n_{ij}$ | $p_{ij}$ | $L_{ij}$ | $N_j$ | $P_j$ | $G_j$ | $U_j$ |
| $PC_1$ | Sealant sag | 0.0240 | 0.0240 | 0.0676 | | | | |
| | Sealant for cracking | 0.0015 | 0.0024 | 0.0056 | 0.0557 | 0.0394 | 0.2404 | 0.0966 |
| | Glue overflow | 0.0302 | 0.0130 | 0.0610 | | | | |
| $PC_2$ | Glass cracks | 0.0069 | 0.0122 | 0.0273 | | | | |
| | Lens mura | 0.0199 | 0.0020 | 0.0313 | 0.0327 | 0.0252 | 0.0051 | 0.0931 |
| | Chamfering fragment | 0.0059 | 0.0110 | 0.0242 | | | | |
| $PC_3$ | Extrusion light leakage | 0.0022 | 0.0037 | 0.0085 | | | | |
| | Sealant light leakage | 0.0180 | 0.0120 | 0.0426 | 0.0402 | 0.0520 | 0.2332 | 0.0947 |
| | Leakage flow on line | 0.0200 | 0.0363 | 0.0790 | | | | |
| $PC_4$ | Waving | 0.0093 | 0.0097 | 0.0272 | 0.0189 | 0.0193 | 0.0001 | 0.0929 |
| | Bad opening | 0.0096 | 0.0096 | 0.0274 | | | | |
| $PC_5$ | Cell foreign body | 0.0180 | 0.0252 | 0.0610 | | | | |
| | Incoming burst | 0.0030 | 0.0048 | 0.0112 | 0.0296 | 0.0446 | 0.1669 | 0.0983 |
| | Foreign film | 0.0086 | 0.0146 | 0.0331 | | | | |
| $PC_6$ | IC high temperature | 0.0100 | 0.0030 | 0.0186 | 0.0304 | 0.0234 | 0.2023 | 0.0827 |
| | IC poor, broken | 0.0204 | 0.0204 | 0.0577 | | | | |
| $PC_7$ | FPC poor, broken | 0.0232 | 0.0232 | 0.0654 | 0.0312 | 0.0312 | 0.1787 | 0.0837 |
| | FPC foreign matter | 0.0080 | 0.0080 | 0.0229 | | | | |
| $PC_8$ | BLU foreign matter | 0.0040 | 0.0071 | 0.0159 | | | | |
| | NG of BLU | 0.0240 | 0.0124 | 0.0516 | 0.0617 | 0.0549 | 0.1832 | 0.0974 |
| | Joint NG | 0.0337 | 0.0354 | 0.0964 | | | | |
| $PC_9$ | TP function NG | 0.0014 | 0.0023 | 0.0053 | | | | |
| | Scrap collection | 0.0050 | 0.0054 | 0.0149 | | | | |
| | Round hole not round, | 0.0025 | 0.0035 | 0.0086 | 0.0260 | 0.0386 | 0.4453 | 0.1371 |
| | fragments | 0.0021 | 0.0036 | 0.0082 | | | | |
| | TP raw material NG | 0.0150 | 0.0238 | 0.0549 | | | | |

| PCs | | | | | | | | |
|---|---|---|---|---|---|---|---|---|
| | Bright spot | 0.0200 | 0.0340 | 0.0759 | | | | |
| | Nuclear white ball | 0.0131 | 0.0233 | 0.0516 | | | | |
| $PC_{10}$ | Appearance of HL | 0.0052 | 0.0097 | 0.0213 | 0.0898 | 0.1225 | 0.0533 | 0.1135 |
| | Joint offset | 0.0360 | 0.0270 | 0.0881 | | | | |
| | Vertical line | 0.0155 | 0.0285 | 0.0621 | | | | |

Note: IC Integrated circuit; BLU backlight unit; NG not good; TP touch panel; HL horizontal line

Table 7 Description of *RFs* of *FMs*

| PCs | FMs | $FM_{jv}$ | S | O | D |
|---|---|---|---|---|---|
| $PC_1$ | Pasting bubbles | $FM_{11}$ | VH | VL | H |
| $PC_2$ | Broken screen | $FM_{21}$ | VH | M | M |
| $PC_3$ | Color tolerance | $FM_{31}$ | M | L | H |
| $PC_4$ | Notch cracks | $FM_{41}$ | M | H | L |
| | Color differences | $FM_{42}$ | H | M | L |
| $PC_5$ | White screen deviation | $FM_{51}$ | L | VL | H |
| | Gamma offset | $FM_{52}$ | H | H | L |
| | Residual shadow | $FM_{53}$ | H | L | H |
| $PC_6$ | ESD damage | $FM_{61}$ | VH | L | VL |
| | Flicker | $FM_{62}$ | H | L | L |
| | Power consumption problem | $FM_{63}$ | H | L | L |
| $PC_7$ | FPC line break | $FM_{71}$ | VH | M | H |
| | FPC fracture | $FM_{72}$ | VH | VL | L |
| | FPC assembly deviation | $FM_{73}$ | VH | VL | L |
| | IC pin off | $FM_{74}$ | VH | M | H |
| $PC_8$ | BLU size deviation | $FM_{81}$ | H | VL | L |
| | Film warping | $FM_{82}$ | H | L | H |
| | Edge bright line | $FM_{83}$ | H | VL | L |
| | Unsuitable LED selection | $FM_{84}$ | H | VL | H |
| $PC_9$ | Offset light leakage | $FM_{91}$ | M | L | H |
| | LED off light | $FM_{92}$ | H | M | L |
| | Improper tray | $FM_{93}$ | H | L | VL |
| | Fragments | $FM_{94}$ | H | M | H |
| | Reversed FPC connection | $FM_{95}$ | H | VL | VL |
| | Foreign bodies in the drum | $FM_{96}$ | H | L | M |
| $PC_{10}$ | Bad point line | $FM_{101}$ | VH | H | VL |
| | Picture flicker | $FM_{102}$ | H | L | VL |
| | Extrusion light leakage | $FM_{103}$ | M | H | H |
| | Power consumption problem | $FM_{104}$ | H | L | M |
| | Dark line | $FM_{105}$ | VH | H | VL |
| | Serrated display | $FM_{106}$ | H | VL | L |

## Acknowledgements

**Declarations**

**Author contributions**: Xiaozhen Lian performed the data analyses and wrote the manuscript, the main idea of the article, and the conclusion analysis of the article. Liang Hou was responsible for the overall understanding of the structure of the article. Wenbo Zhang and Huasheng Yan performed the data analyses. Ying Liu performed revision of the full text.

**Conflict of interest**: No potential conflict of interest was reported by all authors.

**Ethical approval**: This article does not contain any studies with human participants or animals performed by any of the authors.

**Informed consent**: Informed consent was obtained from all individual participants included in the study.

## References

Aguirre García P A, Pérez-Domínguez L, Luviano-Cruz D, et al. (2021) PFDA-FMEA, an integrated method improving fmea assessment in product design. Applied Sciences, 11(4): 1406. https://doi.org/10.3390/app11041406.

Belu N., Anghel D. C., and Rachieru N. (2013) Application of fuzzy logic in design failure mode and effects analysis. Applied Mechanics and Materials. Trans Tech Publications Ltd., 371: 832-836.

Bovea M D, Wang B (2007) Redesign methodology for developing environmentally conscious products. International Journal of Production Research, 45(18-19): 4057-4072.

Bhattacharjee, P., Dey, V., & Mandal, U. K. (2022) Failure Mode and Effects Analysis (FMEA) using interval number based BWM-MCDM approach: Risk Expected Value (REV) method. Soft Computing, 1-22. https://doi.org/10.1007/s00500-022-07264-9.

Brenner W, Uebernickel F (2016) Design thinking for innovation. Research and Practice: Springer. pp: 85-102.

Chang, K. H., & Wen, T. C. (2010) A novel efficient approach for DFMEA combining 2-tuple and the OWA operator. Expert Systems with Applications, 37(3), 2362-2370.

Chen SH (2016) Determining the service demands of an aging population by integrating QFD and FMEA method. Quality & Quantity, 50(1): 283-298.

Chutia R, Gogoi M K (2018) Fuzzy risk analysis in poultry farming based on a novel similarity measure of fuzzy numbers. Applied Soft Computing, 66: 60-76.

De Andrade J M M, de M. Leite A F C S, Canciglieri M B, et al. (2022) A multi-criteria decision tool for FMEA in the context of product development and industry 4.0. International Journal of Computer Integrated Manufacturing, 35(1), 36-49.

Deng, X., & Yuan, Y. (2021) A novel fuzzy dominant goal programming for portfolio selection with systematic risk and non-systematic risk. Soft Computing, 25(23): 14809-14828.

Fazeli H R, Peng Q (2021) Integrated approaches of BWM-QFD and FUCOM-QFD for improving weighting solution of design matrix. Journal of Intelligent Manufacturing, 1-18. https://doi.org/10.1007/s10845-021-01832-w.

Filz M A, Langner J E B, Herrmann C, Thiede S (2021) Data-driven failure mode and effect analysis (FMEA) to enhance maintenance planning. Computers in Industry, 129: 103451. https://doi.org/10.1016/j.compind.2021.103451.

Gautam N, Singh N (2008) Lean product development: Maximizing the customer perceived value through design change (redesign). International Journal of production economics, 114(1): 313-332.

Geyer F, Lehnen J, Herstatt C (2018) Customer need identification methods in new product development: what works "best"?. International Journal of Innovation and Technology Management, 15(01): 1850008. https://doi.org/10.1142/S0219877018500086.

Hou L, Jiao R J (2020) Data-informed inverse design by product usage information: a review, framework and outlook. Journal of Intelligent Manufacturing, 31(3): 529-552.

Huang, Q., Wu, G., & Li, Z. S. (2019) Design for reliability through text mining and optimal product verification and validation planning. IEEE Transactions on Reliability, 70(1), 231-247.

Jiao R, Commuri S, Panchal J, Milisavljevic-Syed, J, et al. (2021) Design engineering in the age of industry 4.0. Journal of Mechanical Design, 143(7): 070801. https://doi.org/10.1115/1.4051041.

Kusiak A (2017) Smart manufacturing must embrace big data. Nature News, 544(7648): 23-25. https://doi.org/10.1038/544023a.

Lee J, Ardakani H D, Yang S, Bagheri B (2015). Industrial big data analytics and cyber-physical systems for future maintenance & service innovation. Procedia, 38: 3-7.

Liang D, Li F (2021) Risk Assessment in Failure Mode and Effect Analysis: Improved ORESTE Method With Hesitant Pythagorean Fuzzy Information. IEEE Transactions on Engineering Management. DOI: 10.1109/TEM.2021.3073373.

Li Z S, Kou F H, Cheng X C, Wang T (2006) Model-based product redesign. International Journal of Computer Science and Network Security, 6(1A),100-108.

Lin H, You J, Zhang X. (2021) Supplier selection with different risk preferences and attribute sets: An innovative study based on generalized linguistic term sets, Advanced Engineering Informatics, 50: 101424. https://doi.org/10.1016/j.aei.2021.101424.

Liu H C, Chen Y Z, You J X, Li H (2016a) Risk evaluation in failure mode and effects analysis using fuzzy digraph and matrix approach. Journal of Intelligent Manufacturing, 27(4): 805-816.

Liu S F, Cheng J H, Lee Y L, Gau F R (2016b). A case study on FMEA-based quality improvement of packaging designs in the TFT-LCD industry. Total Quality Management & Business Excellence, 27(3-4): 413-431.

Ma H, Chu X, Xue D, Chen D (2017) A systematic decision making approach for product conceptual design based on fuzzy morphological matrix. Expert Systems with Applications, 81: 444-456.

Ma H, Chu X, Xue D, Chen D (2019). Identification of to-be-improved components for redesign of complex products and systems based on fuzzy QFD and FMEA. Journal of Intelligent Manufacturing, 30(2): 623-639.

Molla M U, Giri B C, Biswas P (2021) Extended PROMETHEE method with Pythagorean fuzzy sets for medical diagnosis problems. Soft Computing, 25(6): 4503-4512.

Mu R, Zheng Y, Zhang K, Zhang Y (2021) Research on Customer Satisfaction Based on Multidimensional Analysis. International Journal of Computational Intelligence Systems, 14(1), 605-616.

Provost F, Fawcett T (2013) Data science and its relationship to big data and data-driven decision making. Big data, 1(1): 51-59.

Rivera Torres, P. J., Serrano Mercado, E. I., & Anido Rifón, L. (2018) Probabilistic Boolean network modeling and model checking as an approach for DFMEA for manufacturing systems. Journal of Intelligent Manufacturing, 29(6), 1393-1413.

Safari H, Faraji Z, Majidian S (2016) Identifying and evaluating enterprise architecture risks using FMEA and fuzzy VIKOR. Journal of Intelligent Manufacturing, 27(2): 475-486.

Sellappan, N., Nagarajan, D., & Palanikumar, K. (2015) Evaluation of risk priority number (RPN) in design failure modes and effects analysis (DFMEA) using factor analysis. International Journal of Applied Engineering Research, 10(14): 34194-34198.

Selvachandran G, Garg H, Alaroud M H, Salleh A R (2018) Similarity measure of complex vague soft sets and its application to pattern recognition. International Journal of Fuzzy Systems, 20(6): 1901-1914.

Serrano-Guerrero J, Olivas J A, Romero F P, & Herrera-Viedma E (2015) Sentiment analysis: A review and comparative analysis of web services. Information Sciences, 311: 18-38.

Shin J H, Kiritsis D, Xirouchakis P (2015) Design modification supporting method based on product usage data in closed-loop PLM. International Journal of Computer Integrated Manufacturing, 28(6): 551-568.

Smith S, Smith G, Shen Y T (2012) Redesign for product innovation. Design Studies, 33(2): 160-184.

Smith S, Smith G C, Chen Y R (2013) A KE-LSA approach for user-centered design. Journal of Intelligent Manufacturing, 24(5): 919-933.

Sun S Y, Zhu H m (2017) PROMETHEE's parameters setting method based on robustness analysis. Systems Engineering and Electronics, 39(1):120-124(in Chinese).

Tang L, Meng Y (2021) Data analytics and optimization for smart industry. Frontiers of Engineering Management, 8(2): 157-171.

Tian Z P, Wang J Q, Zhang H Y (2018) An integrated approach for failure mode and effects analysis based on fuzzy best-worst, relative entropy, and VIKOR methods. Applied Soft Computing, 72: 636-646.

Van Waarde H J, Eising J, Trentelman H L, Camlibel M K (2020) Data informativity: a new perspective on data-driven analysis and control. IEEE Transactions on Automatic Control, 65(11): 4753-4768.

Wang W Z, Liu X W, Liu S L (2019) Failure mode and effect analysis for machine tool risk analysis using extended gained and lost dominance score method. IEEE Transactions on Reliability, 69(3): 954-967.

Wan S P, Dong J Y (2015) Interval-valued intuitionistic fuzzy mathematical programming method for hybrid multi-criteria group decision making with interval-valued intuitionistic fuzzy truth degrees. Information Fusion, 26: 49-65. https://doi.org/10.1016/j.inffus.2015.01.006.

Wu X, Liao H (2021) Customer-oriented product and service design by a novel quality function deployment framework with complex linguistic evaluations. Information Processing & Management, 58(2): 102469. https://doi.org/10.1016/j.ipm.2020.102469.

Xia H C, Li D F, Zhou J Y, Wang J M (2006) Fuzzy LINMAP method for multi attribute decision making under fuzzy environments. Journal of Computer and System Sciences, 72(4): 741-759.

Xia Y, Tan D, Wang B (2021) Use of a product service system in a competing remanufacturing market. Omega, 102: 102387. https://doi.org/10.1016/j.omega.2020.102387.

Xu Q, Jiao R J, Yang X, Helander M, Khalid H M, Opperud A (2009) An analytical Kano model for customer need analysis. Design studies, 30(1): 87-110.

Yan H B, Ma T (2015) A group decision-making approach to uncertain quality function deployment based on fuzzy preference relation and fuzzy majority. European Journal of Operational Research, 241(3): 815-829.

Yu J X, Wu S B, Chen H C, Yu Y, et al. (2021) Risk assessment of submarine pipelines using modified FMEA approach based on cloud model and extended VIKOR method. Process Safety and Environmental Protection, 155: 555-574.

Yucesan M, Gul M (2021) Failure modes and effects analysis based on neutrosophic analytic hierarchy process: method and application. Soft Computing, 25: 11035-11052.

Zhang L, Chu X, Xue D (2019) Identification of the to-be-improved product features based on online reviews for product redesign. International Journal of Production Research, 57(8): 2464-2479.

Zhang H, Rao H, Feng J (2018) Product innovation based on online review data mining: a case study of Huawei phones. Electronic Commerce Research, 18(1): 3-22.

Zhang W, Wang S J, Hou L, et al. (2021) Operating data-driven inverse design optimization for product usage personalization with an application to wheel loaders. Journal of Industrial Information Integration, 23: 100212. https://doi.org/10.1016/j.jii.2021.100212.

Zhang Z, Chu X (2011) Risk prioritization in failure mode and effects analysis under uncertainty. Expert Systems with applications, 38(1): 206-214.

Zheng L, He Z, He S (2021) An integrated probabilistic graphic model and FMEA approach to identify product defects from social media data. Expert Systems with Applications, 178: 115030. https://doi.org/10.1016/j.eswa.2021.115030.

Zhou J, Liu Y, Xiahou T, Huang T (2021) A Novel FMEA-Based Approach to Risk Analysis of Product Design Using Extended Choquet Integral. IEEE Transactions on Reliability, 1-17. DOI:10.1109/TR.2021.3060029.

Zhou F, Ji Y, Jiao R J (2013) Affective and cognitive design for mass personalization: status and prospect. Journal of Intelligent Manufacturing, 24(5): 1047-1069.